
Adversarial Learning and Explainability in Structured Datasets

Prasad Chalasani

MediaMath

New York, NY

pchalasani@gmail.com

Somesh Jha

University of Wisconsin, Madison

jha@cs.wisc.edu

Aravind Sadagopan

MediaMath

New York, NY

arvind.contactme@gmail.com

Xi Wu

Google

Madison, WI

wu.andrew.xi@gmail.com

Abstract

We theoretically and empirically explore the explainability benefits of adversarial learning in logistic regression models on structured datasets. In particular we focus on improved explainability due to significantly higher *feature-concentration* in adversarially-learned models: Compared to natural training, adversarial training tends to more efficiently shrink the weights of non-predictive and weakly-predictive features, while model performance on natural test data only degrades slightly (and even sometimes improves), compared to that of a naturally trained model. We provide theoretical insight into this phenomenon via an analysis of the expectation of the logistic model weight updates by an SGD-based adversarial learning algorithm, where examples are drawn from a random binary data-generation process. We empirically demonstrate the feature-pruning effect on a synthetic dataset, some datasets from the UCI ML Repository [1], and real-world large-scale advertising response-prediction data-sets from MediaMath. In several of the MediaMath datasets there are 10s of millions of data points, and on the order of 100,000 sparse categorical features, and adversarial learning often results in model-size reduction by a factor of 20 or higher, and yet the model performance on natural test data (measured by AUC) is comparable to (and sometimes even better) than that of the naturally trained model. We also show that traditional ℓ_1 regularization does not even come close to achieving this level of feature-concentration. We measure "feature concentration" using the Integrated Gradients-based feature-attribution method of [2] and derive a new closed-form expression for 1-layer networks, which substantially speeds up computation of aggregate feature attributions across a large dataset.

1 Introduction

While deep learning models have been wildly successful in a variety of perceptual (images, audio, video) and text domains, a number of authors have recently highlighted two important concerns with such models:

- **Adversarial Examples:** Many of these models are vulnerable to *adversarial attacks*: it is possible for an adversary to perturb the inputs in such a way that humans perceive no significant change (and in particular they would assign the same "label" as the original example), and yet the model's label or prediction can be markedly different [3, 4]. *Adversarial training*

has recently been proposed as a method for training models that are robust to such attacks, by applying techniques from the area of Robust Optimization [5–7].

- **Feature Attribution:** Especially for complex models, but even for simple linear models, it is often not clear how to quantify the impact of an input feature on the model’s final output. Such a quantification is crucial in order to understand which features are relevant (and irrelevant or marginally relevant) in determining a model’s behavior on specific inputs, or to understand which features are important in aggregate. This understanding can highlight a model’s strengths or weaknesses and can aid in improving the models or help instill trust in the models (especially in domains such as health-care). A few different feature attribution techniques have been proposed recently [8, 9], and [10, 11] are two recent surveys of various explanation methods for black-box models. In particular [2] formulate a set of axioms that any good feature-attribution method should satisfy and identify a specific method, which they call Integrated Gradients (IG) that satisfies all of these axioms.

Much of the recent work on Adversarial Machine Learning (AML) has focused on perceptual domains or text, and "structured" datasets have been largely ignored. (For all practical purposes, structured datasets can be thought of as tabular datasets such as those arising from health-care, advertising, or a variety of other application areas, where the values in the table columns are numerical or categorical). Moreover, AML research has been primarily concerned with producing adversarially robust models, and the conventional wisdom is that adversarial robustness comes at the cost of (often significant) loss in classification performance on natural examples [12–14].

For example, in [15] the authors create a synthetic dataset where they demonstrate a tradeoff between *standard accuracy* (i.e. accuracy on natural unperturbed examples), and *adversarial accuracy* (i.e. accuracy on adversarially perturbed examples). In particular, on their synthetic dataset, they show that as standard accuracy approaches 100%, adversarial accuracy falls to zero. Other tradeoffs have also been considered in the literature, such as the need for more training data to achieve adversarial robustness [16].

The emphasis in this paper is different in a few ways. We explore adversarial training, not in perceptual or text domains, but in *structured datasets*. Our primary interest in this paper is not adversarial robustness or adversarial accuracy, but rather an intriguing side-benefit of adversarial training:

Adversarial training (with ℓ_∞ -bounded perturbations) can be used to produce models significantly *more concentrated* than their naturally-trained counterparts, with *minimal or no impact on standard accuracy* (i.e. the performance on natural data), particularly in logistic probability-prediction models applied to structured datasets. Moreover, this effect is not achievable by traditional ℓ_1 -regularization.

We use the term feature-concentration (or "model compression", or "model concentration") informally to refer to the extent to which the learned model differentiates between "relevant" and "less relevant" or "irrelevant" features. (See below for more on measuring feature concentration). An aspect of adversarial training that we are especially interested in, is its ability to weed out (the weights of) non-predictive features that exhibit spurious correlation with the label on finite datasets. This is clearly important from an *explainability* viewpoint: We would like our trained model to not place significant weights on such irrelevant features.

It is now standard [6] to view adversarial training as a process similar to the usual model-training where a certain loss function is minimized, except that each d -dimensional input instance x is altered by an adversary by adding a d -dimensional perturbation δ to x , where the adversary chooses $\delta = \delta^*$ in the "worst" possible way given the current model state and certain constraints (a formal description appears in Section 3.1). The constraint on the adversary is typically in the form of a bound ε on the ℓ_∞ -norm of δ . For brevity we will refer to such an adversary as a $\ell_\infty(\varepsilon)$ adversary. The key difficulty in scaling up adversarial training to large datasets is the computation of this worst-case δ^* at each input sample point. For a general model there is often no choice but to apply an iterative optimization procedure, such as Projected Gradient Descent (PGD), at each sample point to compute the worst-case perturbation δ^* . However for linear models (such as logistic or poisson) we derive a simple closed-form expression (Lemma 3.1 in Section 3.1) for δ^* under ℓ_∞ -norm and ℓ_2 -norm constraints. This result makes it practical to incorporate adversarial training into a learning system based on logistic or other linear models.

Theorem 3.1 in Section 3.2 is our main theoretical result that sheds light on the feature-concentration effect of adversarial training. This result gives bounds on the *expectation* of the logistic weight updates when a Stochastic Gradient Descent (SGD) algorithm is applied to data points from an idealized data-generation process, that are subjected to the worst-case $\ell_\infty(\varepsilon)$ -adversarial perturbation according to the closed-form expression mentioned above. These bounds show a clear link between the expected SGD update of a feature's weight, and the relative magnitudes of ε and the (absolute) *label-correlation* of the feature (i.e. the correlation between the feature and the label). Roughly speaking, for features whose absolute label-correlations are *less* than ε , the SGD updates on average tend to *shrink* their weights toward zero, at a rate proportional to the difference between ε and the label-correlation. On the other hand, for features whose absolute label-correlations are sufficiently *larger* than ε , the SGD updates on average tend to *expand* their weights in their current direction.

This suggests that $\ell_\infty(\varepsilon)$ -adversarial training with an appropriate value of ε acts as a *relevance filter* that weeds out the weights of irrelevant or weakly-relevant features, while preserving weights of relevant features, such that standard accuracy is only minimally sacrificed. In fact if there is a large gap between the absolute label-correlations of "relevant" features and those of "irrelevant" features, then this result suggests the existence of a "*goldilocks zone*" of ε values that are "just right": large enough to suppress irrelevant or weakly-relevant features, and yet small enough to preserve relevant features such that standard accuracy is not impacted significantly. This is precisely the phenomenon we observe in several experimental studies on synthetic, toy, large-scale real-world datasets, as described below. A more detailed description of the implications of Theorem 3.1 appears in Section 3.3.

Inspired by the synthetic dataset of [15], we define a synthetic dataset (Section 4) expressly designed to dramatically highlight the contrast between adversarial training and natural training in their ability to ignore irrelevant features. In contrast to the theoretical analysis of [15], we conduct SGD-based adversarial training experiments on this dataset. Our synthetic dataset contains a mix of predictive and purely random non-predictive features, and natural training tends to learn significant weights on the non-predictive features (with the weights sometimes being bigger than those of the predictive features), whereas adversarial training acts as an efficient sieve that weeds out the non-predictive features by pushing their weights close to zero, while still leaving the predictive features with significant weights, hence only minimally impacting (and sometimes even improving) standard accuracy.

How do we quantify feature concentration? One possibility, applicable to linear models, is based on the weights of the features (see the measures Wts.L1 and Wts.1Pct defined in Section 6.1). We also consider concentration measures using the more principled Integrated Gradients (IG) based approach of [2]. Specifically we compute each feature's "importance" using the IG methodology, and then measure "concentration" based on how this measure varies across features (see Section 6.1 for details).

The core of the IG method is an expression for the contribution of a given feature-dimension i to a specific prediction $p(x)$ on an input sample x . This expression involves a line integral over gradients computed along the straight-line path from a certain baseline input x' to the actual input x . Computing this integral in general requires an approximation based on gradients computed at m equally spaced points on this straight-line path. This is reasonably efficient to compute for a single datapoint x and single dimension i . However in this paper we are interested in repeatedly computing this quantity across all dimensions (which could number into the hundreds of thousands when there are high-cardinality categorical features), over an entire dataset (which could contain millions of records). Fortunately, we are able to show a closed-form formula for the IG-based attribution for 1-layer neural networks with an *arbitrary* differentiable activation function (Lemma 5.1 in Section 5.1).

While the IG methodology of [2] focuses on feature-attribution for a single sample point, for our purposes we also want to quantify the overall importance of a feature in a model, aggregated over a specific dataset. In Section 5.2 we introduce a simple, intuitive methodology to compute such an aggregate feature-importance metric we call the *Feature Impact*.

In Sections C and 6.2 we describe our experiments on toy datasets from the UCI repository [1], and large scale real-world advertising datasets from MediaMath respectively. In these experiments we compare results from natural training and adversarial training where the adversary's perturbations δ are constrained such that $\|\delta\|_\infty < \varepsilon$ for some positive ε . The common theme that emerges

from these experiments is that there is almost always a "goldilocks zone" for ε where ε is large enough to cause significant feature-concentration, yet small enough not to damage performance (as measured by AUC or accuracy) on natural test data. We also study whether this type of model-concentration/performance-preservation effect can be achieved using traditional ℓ_1 regularization. We find that on the toy UCI or synthetic datasets we are forced to use a very large ℓ_1 regularization parameter λ (more than 200 for example) to achieve this effect, whereas on the real-world MediaMath datasets, this effect cannot be achieved at all with ℓ_1 regularization: When λ is large enough to produce a model concentration comparable to adversarial training, the AUC is much worse, while a smaller lambda that preserves AUC produces a much inferior model concentration.

To summarize, our main contributions are:

- A novel theoretical analysis (Theorem 3.1) of the expectation of SGD updates of logistic regression model weights during $\ell_\infty(\varepsilon)$ adversarial training (on data points from an idealized random data generation process), that shows that adversarial learning acts as an *aggressive relevance filter*: on average the weight of a feature shrinks or expands depending on whether its absolute label-correlation is smaller than ε or (sufficiently) larger than ε respectively. One implication of the result is that when there is a large gap between the absolute label-correlations of relevant and irrelevant (or weakly-relevant) features, then ε values in this gap region constitute a *goldilocks zone* for model-concentration: in this zone ε is "just right": large enough to shrink weights of irrelevant features, and small enough to preserve or expand weights of relevant features, thus only minimally impacting standard accuracy (or AUC-ROC).
- Experimental results (Sections 4, C, 6.2) showing that $\ell_\infty(\varepsilon)$ -adversarial training of logistic regression models (on synthetic data, UCI data, and large-scale real-world advertising datasets from MediaMath) exhibits the above relevance-filtering phenomenon, with a goldilocks zone of ε values. When there are a large number of low-relevance features, this aggressive relevance-filtering results in models that are significantly more *concentrated* than their naturally-trained counterparts, without significantly sacrificing standard accuracy. In particular on some of the MediaMath datasets we show that with $\ell_\infty(\varepsilon)$ -adversarial training using $\varepsilon = 0.01$, the number of significant absolute weights (i.e. those within 1% of the largest absolute weight) drops by a factor of 20, while the AUC-ROC on natural test data is nearly the same as with $\varepsilon = 0$ (i.e. natural training). We also show that traditional ℓ_1 -regularization cannot be used to achieve this type model-concentration while preserving standard accuracy.
- A closed form formula (Lemma 5.1) for the Integrated Gradients-based Feature Attribution of [2] for 1-layer neural networks with an *arbitrary* differentiable activation function (of which logistic models are a special case), and the use of this formula to efficiently compute new measures of feature-importance and model-concentration on a dataset.

2 Background, Definitions and Notation

For ease of reference, in this section we collect some basic terminology, concepts and known results pertaining to Machine Learning, Neural Network models, Adversarial Training, and Feature Attribution.

2.1 Machine Learning Datasets and Binary Probability-Prediction

We are interested in machine-learning tasks in domains where the primary emphasis is in developing models that predict the *probability* of the event. Such models are useful in a wide variety of areas, for instance in advertising to predict response-rates from ad exposure[17, 18], and in health-care to predict the probability of adverse events[19]. In advertising, the probability is directly used to determine the best price to bid for an ad opportunity in a real-time-bidding system. This is in contrast to domains considered in much of the adversarial learning literature, where the emphasis is primarily on the *classification* produced by the model.

In this paper we focus on *structured datasets*. For our purposes a structured dataset is one which can be thought of as a table with columns, where the values in the columns can be numerical or categorical. We assume categorical features are "1-hot encoded" (as described in the next subsection) at least implicitly if not explicitly.

A *training dataset* \mathcal{D} consists of example-label pairs (x, y) where $x \in \mathbb{R}^d$ is a d -dimensional example vector and $y \in \{+1, -1\}$ is the corresponding binary label¹, where $y = 1$ indicates the occurrence of an event of interest. When a model is trained on dataset \mathcal{D} , the output $F(x)$ of the model for an input x is interpreted as the predicted probability that $y = 1$. Throughout the paper, it is assumed that the input vector x represents the "exploded" feature vector where each categorical feature in the original example has been 1-hot encoded, as described in the next subsection (see more on this in the next sub-section).

2.2 One-hot Encoding of Categorical Features

In ad conversion prediction and other domains involving structured datasets, several (or even most) features can be categorical. We introduce some notation and terminology to simplify the description of some of our results involving categorical features in Section 5.2.

An example vector in *original* form (i.e. prior to one-hot encoding of categorical features) is denoted u , and u_k refers to the k 'th feature (which could be numerical or categorical). If feature u_k is categorical, then V_k denotes the set of possible values of the feature, i.e. V_k represents the "vocabulary" of this feature. The *cardinality* of feature u_k is $m_k := |V_k|$. We assume that V_k is in *index* form, i.e. regardless of what the actual feature values are, we assume they are represented as indices in $[m_k] := \{1, 2, \dots, m_k\}$. For example if u_k is the `dayOfWeek` feature, it has the 7 possible values $V_k = [7] = \{1, 2, \dots, 7\}$, and its cardinality m_k is 7. Sometimes cardinalities can be much larger. For example in the advertising datasets we study in our experiments, a website URL is encoded as an integer `siteID`, which has cardinality around 50,000.

For a categorical feature u_k , its *1-hot representation* is denoted h_k and is obtained by starting with an m_k -dimensional vector of all zeros, and setting dimension i to 1, where i is the value of u_k . For example if $u_k = 2$ and its cardinality $m_k = 4$, then h_k is the vector $\langle 0, 1, 0, 0 \rangle$. For notational convenience, for a numerical feature u_k , we let $h_k = u_k$ denote its "one-hot encoding", which is identical to u_k . For a feature-vector (in original form) $u = [u_1, u_2, \dots, u_d]$, we let x represent the vector resulting from concatenating the 1-hot encoding h_k of each u_k in the natural way:

$$x = [h_1, h_2, \dots, h_d] \quad (1)$$

We then say that x is in *exploded form*. For example suppose $u = [u_1, u_2, u_3]$ is a 3-dimensional feature vector in original form, u_1 is categorical with cardinality $m_1 = 3$, u_2 is numerical, and u_3 is categorical with cardinality $m_3 = 2$. If $u = \langle 2, 3.5, 1 \rangle$, then the exploded form x after 1-hot transformation is:

$$x = [0, 1, 0, 3.5, 1, 0] \quad (2)$$

We use I_k to denote the (contiguous) set of dimensions corresponding to the original feature u_k , in the exploded vector x . In the above example $I_1 = \{1, 2, 3\}$, $I_2 = \{4\}$, and $I_3 = \{5, 6\}$.

2.3 1-Layer Neural Networks

A 1-layer neural network is defined by learnable parameters $w \in \mathbb{R}^d$ (the *weight vector*) and $b \in \mathbb{R}$ (the *bias*), and a differentiable scalar activation function A , and computes the following function for any input feature-vector $x \in \mathbb{R}^d$ (in exploded space):

$$F(x) = A(\langle w, x \rangle + b), \quad (3)$$

where $\langle w, x \rangle$ denotes the dot product of w and x . Although in all of our experiments we train (logistic) models that include the bias b , we do not include the bias b (also called the "intercept") in most of our results; this is without loss of generality since the effect of the bias term can be captured by setting one of the dimensions of the input vector x to 1.0, and the presence of the bias term adds notational clutter but does not meaningfully alter our results.

¹For mathematical convenience we use -1/1 as the labels in the theoretical results, whereas in the experiments we often use 0/1 labels, but these are trivially transformed to -1/1 and the same results apply.

Two commonly used models fall within the class of 1-layer networks: *Logistic* regression models where the activation function A is the sigmoid (or logistic) function $A(z) = \sigma(z) = 1/(1 + e^{-z})$, and *Poisson* regression models where the activation is $A(z) = e^z$. In the case of a logistic model, the value of $F(x)$ will lie in $[0, 1]$ and can be interpreted as a *probability prediction*. Logistic and Poisson models are members of the more general class of Generalized Linear Models [20].

2.4 Natural Training of Logistic Models

Logistic models are typically trained by minimizing the *empirical risk*, expressed as the expected *Negative Log Likelihood (NLL) loss*:

$$\min_w \mathbb{E}[L(x, y; w)], \quad (4)$$

where the NLL loss L is given by:

$$L(x, y; w) := \ln(1 + \exp(-y\langle w, x \rangle)) = -\ln \sigma(y\langle w, x \rangle) \quad (5)$$

Note that the prediction \hat{y} is a function of x and w , so the loss on a given example (x, y) is a function of x, y and w .

2.5 Adversarial Training of Logistic Models

While Empirical Risk Minimization (ERM) has been successfully used in a variety of domains to yield classifiers that perform well on examples drawn from the *natural* data distribution \mathcal{D} , such classifiers have repeatedly been shown to be vulnerable to *adversarially* crafted examples (see [6, 3, 21] and references therein). As a result there has been a growing interest in *adversarial training*, i.e. training models that are robust to adversarial examples. As mentioned in the Section 1, our primary interest in adversarial training is not adversarial robustness but rather in the resulting improved model-concentration (and hence improved model-explainability).

Following [6], for our logistic models and NLL loss, we formulate adversarial learning as the problem of minimizing the *expected adversarial loss*:

$$\mathbb{E}_{(x, y) \sim \mathcal{D}} \left[\max_{\delta \in \Delta} L(x + \delta, y; w) \right], \quad (6)$$

where Δ is the set of possible perturbations to the input x that the adversary is allowed to make.

It is common practice to consider Δ to be the set of ℓ_p -bounded perturbations. For brevity we will use the phrase " $\ell_p(\varepsilon)$ -adversary" to refer to an adversary who is allowed to choose perturbations δ such that $\|\delta\|_p \leq \varepsilon$, and we refer to such perturbations as $\ell_p(\varepsilon)$ perturbations. In the rest of the paper, whenever we use the term "*adversarial*" $\ell_p(\varepsilon)$ perturbation, it should be understood that we are referring to the *worst-case* perturbation δ by an $\ell_p(\varepsilon)$ adversary, for the loss function under consideration (i.e. this perturbation achieves the inner max in Eq. (6)).

Thus minimizing expected adversarial loss results in a min-max (or saddle-point) optimization problem which is computationally demanding for general loss functions L (since for each example one must find the worst-case perturbation that maximizes the loss on that example). Fortunately, for logistic models we show in Section 3.1 that the worst-case δ that achieves the inner maximization has a simple closed form expression, when adversarial perturbations are bounded under ℓ_1 and ℓ_∞ -norms.

2.6 Stochastic Gradient Descent (SGD) in Adversarial Training

Whether to minimize the expected natural loss (4) or adversarial loss (6), it is standard to use variants of Stochastic Gradient Descent (SGD). In this paper we assume the following canonical SGD setup for adversarial training of logistic models with an $\ell_\infty(\varepsilon)$ -adversary (For $\varepsilon = 0$ this reduces to the standard SGD for natural examples).

The weight vector w is initialized to all zeros. After each example (x, y) is encountered (where x is in exploded form, i.e. after 1-hot-encoding all categorical features),

1. The input vector x is subjected to an adversarial $\ell_\infty(\varepsilon)$ perturbation, i.e. x is replaced by $x' := x + \delta^*$ where δ^* is the vector $\delta \in \mathbb{R}^d$ that achieves the inner maximum in (6), which we show (Section 3.1) for logistic models is given by Eq. (12) for an $\ell_\infty(\varepsilon)$ -adversary.

2. The logistic NLL loss $L(x', y; w)$ is computed using Eq. (5),
3. Each component w_i of w is updated according to the gradient of the NLL loss w.r.t. w_i :

$$w'_i = w_i - \eta \frac{\partial L(x', y; w)}{\partial w_i}, \quad (7)$$

where $\eta > 0$ is the learning rate.

2.7 Model Performance Measures: Accuracy, ROC-AUC

In this paper we are mainly interested in probability-prediction models, and so we use the Area Under the ROC Curve (AUC-ROC, or AUC in brief) [22] as our primary measure of model performance. In the synthetic datasets, we also use *accuracy* to measure model performance, and there it should be understood that we treat any prediction above (below) 0.5 as a "positive" ("negative") classification, and accuracy is calculated as the fraction of correctly classified examples in the test dataset.

2.8 Feature Attribution in Neural Networks using Integrated Gradients

The main thrust of this paper is to demonstrate the ability of adversarial training to produce models that are much more *concentrated* than naturally-trained ones, without sacrificing accuracy on natural test data. Model concentration can be measured in terms of the model weights (for example by computing the ℓ_1 -norm of the weights), which is reasonable if there are only numerical features of the same scale, and the model is a 1-layer neural network. However in general the weight of a feature, even in a 1-layer neural network, is not necessarily a good measure of its importance to a model: for instance a numerical feature may have a relatively large *weight*, but on a typical dataset, its absolute *value* may be much smaller than other numerical features, or if it is a categorical feature-value, it may occur very infrequently (and hence its overall importance on a dataset may be relatively small). Therefore a more principled approach to measuring the "importance" of a feature in a model is needed.

Feature attribution refers to the general area of understanding how the output of a neural network is impacted by its input features, and this is important in a variety of contexts. For a neural network that computes a function $F : \mathbb{R}^d \rightarrow \mathbb{R}$, some examples of relevant questions are:

- On a *specific* input x , which features of x are "most responsible" for the value of the output $F(x)$, relative to $F(x')$ for some baseline input x' (such as a black image for image models, or a zero vector for logistic prediction models). Such an understanding can aid in debugging or improving a model's performance. Sample-level attribution can also be used as a rationale for a specific output. Such explanations can help the end-user (e.g. a doctor) understand the strengths and weaknesses of the model.
- In *aggregate* over some dataset, what are the relative importances of the features in determining the network output? If there are categorical features, then this question can be asked either at the level of *feature-values* (i.e. the individual values of each categorical feature, such as the different possible values of the "country" feature), or *features* (i.e. each categorical feature in aggregate, such as "country"). Understanding aggregate-level feature importance can help prune features, or identify bugs where a feature that is expected to be important is not turning out to be important (as measured by the specific attribution method), or vice versa.

The key to a useful feature-attribution is a sound methodology which does not have quirks which obscure the impact of features on the model output. In general it is difficult to evaluate an attribution method, so in a recent paper [2] the authors identify several axioms that any sound attribution method must satisfy, and in particular propose a specific method that satisfies these axioms, which they call *Integrated Gradients* (IG). We adopt this IG method in this paper, and it works as follows. Suppose $F : \mathbb{R}^d \rightarrow \mathbb{R}$ represents the function computed by a neural network. Let $x \in \mathbb{R}^d$ be a specific input, and $x' \in \mathbb{R}^d$ be the baseline input. The IG is defined as the path integral of the gradients along the straight-line path from the baseline x' to the input x . The IG along the i 'th dimension for an input x and baseline x' is defined as:

$$IG_i(x) := (x_i - x'_i) \times \int_{\alpha=0}^1 \partial_i F(x' + \alpha(x - x')) d\alpha, \quad (8)$$

where $\partial_i F(z)$ denotes the gradient of $F(u)$ along the i 'th dimension, at $u = z$.

3 Analysis of SGD Updates in Adversarial Training of Logistic Models

Our aim is to understand the nature of the solution to the $\ell_\infty(\varepsilon)$ -adversarial learning problem (6) for logistic regression models. The biggest difficulty in this optimization problem is the inner maximization, which requires finding the worst-case $\ell_\infty(\varepsilon)$ -adversarial perturbation δ^* on each input x . In general one needs to run a separate optimization procedure (such as Projected Gradient Descent [6]) to find this δ^* , but fortunately for logistic regression models there is a simple closed form expression for δ^* , which we show in Lemma 3.1.

While the closed form expression for δ^* makes the $\ell_\infty(\varepsilon)$ -adversarial training of logistic regression models *computationally* as simple as natural training, gaining an *analytical* insight into the nature of the optimum of (6) is still difficult, especially since there is no known closed-form solution for this optimization problem. Rather than analyzing the final optimum of (6), we instead analyze how an SGD-based optimizer updates the model weights under $\ell_\infty(\varepsilon)$ adversarial perturbations. We assume the standard SGD setup for adversarial training described in Section 2.6.

As a first step toward analyzing the SGD-based weight-updates, we show in Proposition 3.1 a simple expression for the *gradient* of the logistic NLL loss (5) on an example perturbed by an $\ell_\infty(\varepsilon)$ -adversary. Analyzing SGD-based weight updates is still challenging since SGD is a stateful, sequential process, so in Section 3.2 we define an idealized data-generation process (which we call the Biased Coin Process, or BCP) and instead analyze the *expectations* of the SGD updates on $\ell_\infty(\varepsilon)$ -perturbed data points drawn from the BCP, which leads to our main theoretical result, Theorem 3.1.

3.1 Adversarial Perturbations for Logistic Models

The following Lemma gives a closed form formula for the $\ell_p(\varepsilon)$ perturbations under the logistic NLL loss (5) for $p \in \{2, \infty\}$.

Lemma 3.1 (Adversarial $\ell_2(\varepsilon), \ell_\infty(\varepsilon)$ perturbations for logistic models) *For a fixed $x, w \in \mathbb{R}^d$, $y \in \{+1, -1\}$, positive integer p , and $\varepsilon > 0$, define $\Delta_p(\varepsilon)$ as the set of perturbations δ whose ℓ_p norm is bounded by ε :*

$$\Delta_p(\varepsilon) := \{\delta \in \mathbb{R}^d \mid \|\delta\|_p \leq \varepsilon\}, \quad (9)$$

and define the adversarial δ as:

$$\delta_p^*(x, y, w, \varepsilon) := \arg \max_{\delta \in \Delta_p(\varepsilon)} L(x + \delta, y; w), \quad (10)$$

where $L()$ is the logistic NLL loss defined in (5). Then

$$\delta_2^*(x, y, w, \varepsilon) = -\frac{w}{\|w\|_2} \varepsilon y \quad (11)$$

$$\delta_\infty^*(x, y, w, \varepsilon) = -\text{sgn}(w) \varepsilon y \quad (12)$$

Proof: Consider the case $y = +1$ (the case $y = -1$ is analogous). In this case the NLL simplifies to $-\ln(\sigma(\langle w, x + \delta \rangle))$, which is monotonically decreasing function of $\langle w, \delta \rangle$. Hence maximizing $L(x + \delta, y; w)$ is equivalent to minimizing $\langle w, \delta \rangle$. When the ℓ_2 -norm of δ is bounded by ε , $\langle w, \delta \rangle$ is minimized when δ is such that it has ℓ_2 -norm ε and points in the direction opposite to w , which implies the first result by noting that $\frac{w}{\|w\|_2}$ is the unit vector in the direction of w . When the ℓ_∞ -norm of δ is bounded by ε , the lowest value of $\langle w, \delta \rangle$ is achieved when each component of δ has magnitude ε but sign opposite that of the corresponding component of w , which implies the second result. \square

The following Proposition shows an expression for the gradient of the logistic NLL loss $L(x + \delta^*, y; w)$ where δ^* is the $\ell_\infty(\varepsilon)$ perturbation (12). The proof, shown in Appendix A, involves simple algebra and applications of the chain rule, and properties of the sigmoid function.

Proposition 3.1 (Gradient of Logistic NLL Loss under $\ell_\infty(\varepsilon)$ adversarial perturbation) *If L is the logistic NLL loss given by (5), and $x' = x + \delta^*$ where δ^* is the $\ell_\infty(\varepsilon)$ adversarial perturbation (12), then for each $i \in [d]$ the gradient $\partial L(x', y; w)/\partial w_i$ is given by:*

$$\frac{\partial L(x', y; w)}{\partial w_i} = -\sigma(\varepsilon \|w\|_1 - y \langle x, w \rangle)(yx_i - \varepsilon \text{sgn}(w_i)) \quad (13)$$

3.2 Expectation of SGD Updates on Adversarially Perturbed BCP data

Since SGD is inherently a stateful process, it is challenging to analyze its sequential dynamics. Instead we analyze the *expectation* of the gradient updates from an arbitrary state, when the training data points (x, y) are drawn from an idealized, general data-generation process we call the *Biased Coins Process* (BCP), defined below. The BCP can be viewed as a generative model that is simulating the distribution of points when drawn with replacement from an actual (finite) dataset. Our main result is Theorem 3.1 which characterizes the expected gradient updates on $\ell_\infty(\varepsilon)$ -adversarially perturbed BCP inputs. This result yields several insights that help explain our results on synthetic datasets (Section 4), the UCI datasets (Section C) and real-world advertising datasets (Section 6.2).

In the BCP, a data-point (x, y) is generated as follows. The label y is chosen uniformly at random from $\{-1, 1\}$, and x is a d -dimensional feature vector where for each $i \in [d]$,

$$x_i = \begin{cases} y & \text{w.p. } 0.5 + b_i \\ -y & \text{w.p. } 0.5 - b_i, \end{cases} \quad (14)$$

where $b_i \in [-0.5, 0.5]$ is the *bias* of feature x_i . Note that $\mathbb{E}(y) = 0$ and for any $i \in [d]$, $\mathbb{E}(x_i) = 0$ and $\mathbb{E}(yx_i) = 2b_i$, and the variance of x_i and y are both 1.0, so the *correlation* of x_i and y is $2b_i$. This fact will be useful when interpreting the implications of Theorem 3.1 in Section 3.3.

Consider an arbitrary stage of the SGD algorithm where the current weight vector is w , and we generate a data-point (x, y) according to the BCP, and after replacing the feature-vector x with $x' = x + \delta^*$ where δ^* is the $\ell_\infty(\varepsilon)$ adversarial perturbation in Eq. (12), we present (x', y) to the SGD algorithm. We then ask what is the *expectation of the gradient-based update* of the weight w_i ? Each w_i will be updated to a new value $w_i - \eta \partial L(x', y; w) / \partial w_i$, where $\eta > 0$ is the (current) learning rate, and L is the logistic NLL loss defined in Eq. (5). For brevity we denote the *change* in w_i by Δw_i , i.e.

$$\Delta w_i := -\eta \frac{\partial L(x', y; w)}{\partial w_i} \quad (15)$$

Given the expression (13) for the gradient of w_i from Proposition 3.1, it turns out that the following conditional expectation will be useful when computing $\mathbb{E}\Delta w_i$:

$$\bar{\sigma}_i(s) := \mathbb{E}[\sigma(\varepsilon\|w\|_1 - y\langle w, x \rangle) \mid yx_i \text{sgn}(w_i) = s], \quad s \in \{\pm 1\}, \quad (16)$$

where the expectation is over data points (x, y) generated by the BCP. Note that the value of $yx_i \in \{\pm\}$ represents whether or not the value of feature x_i is "aligned" with the label y , and $yx_i \text{sgn}(w_i) = 1$ means that the weight of feature x_i is "consistent" with its label-alignment: i.e. either $yx_i = 1$ and $\text{sgn}(w_i) > 0$, or $yx_i = -1$ and $\text{sgn}(w_i) < 0$. Conversely, $yx_i \text{sgn}(w_i) = -1$ means that the weight of feature x_i is "inconsistent" with its label-alignment. In general when $yx_i \text{sgn}(w_i) = s$ we say that "feature x_i has *consistency* s ". Further note that $\sigma(\varepsilon\|w\|_1 - y\langle w, x \rangle)$ is the model's predicted probability of the *wrong* label $-y$ (on an $\ell_\infty(\varepsilon)$ -adversarially perturbed point data-point $x' = x - y\varepsilon \text{sgn}(w)$). We can therefore interpret $\bar{\sigma}_i(s)$ as the "expected mis-prediction, given consistency s of feature x_i ". Intuitively, the value of $\bar{\sigma}_i(s)$ is inversely related to the model's performance on the "slice" of the BCP data where the feature x_i has consistency s . Therefore in the initial stages of the SGD algorithm, we expect $\bar{\sigma}_i(s)$ to be relatively large (i.e. closer to 1.0) and in the later stages, it will relatively small. This intuition will be useful later in Section 3.3 when we interpret the results of Theorem 3.1, which we state below (see Appendix B for the proof).

Theorem 3.1 (Expectation of logistic gradient update for the BCP) *Given a weight vector $w \in \mathbb{R}^d$, assuming a learning rate $\eta = 1$ (only to avoid notational clutter), if a data point (x, y) is drawn according to the BCP above, and $x' = x + \delta^*$ where δ^* is the $\ell_\infty(\varepsilon)$ adversarial perturbation given by Eq. (12), then for each $i \in [d]$, the expectation (over random draws from the BCP) of the SGD update Δw_i (defined in Eq. (15)) satisfies the following properties:*

1. If $w_i = 0$ then

$$\mathbb{E}\Delta w_i = 2b_i \bar{\sigma}_i(1) = 2b_i \bar{\sigma}_i(-1). \quad (17)$$

2. If $w_i \neq 0$, then

$$\text{sgn}(w_i) \mathbb{E}\Delta w_i \leq \bar{\sigma}_i(1)(2 \text{sgn}(w_i) b_i - \varepsilon) \quad (18)$$

and

$$\text{sgn}(w_i) \mathbb{E}\Delta w_i \geq \bar{\sigma}_i(1) [2b_i \text{sgn}(w_i) - |w_i| - \varepsilon(1 + |w_i|)] \quad (19)$$

It is easy to verify from Eq. (15) that when the learning rate $\eta \neq 1$, it shows up as a multiplicative factor on the right hand side of equation (17), and the bounds (18) and (19) in the Theorem.

3.3 Implications of the Expected Gradient Results

Theorem 3.1 has a few interesting implications. It will help to recall from Section 3.2 that the conditional expectation $\bar{\sigma}_i(s)$ can be interpreted as the "expected mis-prediction of the model when feature x_i has consistency s ", which in turn means that in the initial stages of SGD we expect $\bar{\sigma}_i(s)$ to be relatively large, and it will shrink as SGD progresses toward a better model. Since this factor appears in all of the bounds of Theorem 3.1, the various effects discussed below are more pronounced in the initial stages of SGD and less so during later stages. Note also that the quantity $2|b_i|$ appearing in Theorem 3.1 (and in the implications below) is the absolute correlation between x_i and y , as noted at the beginning of Section 3.2. We will refer to $2|b_i|$ as the *absolute label-correlation* of x_i .

In the following interpretations, we say the weight w_i of a feature x_i is *aligned*, if $\text{sgn}(w_i)\text{sgn}(b_i) = 1$, and otherwise we say it is *mis-aligned*. We also informally say that the feature x_i is "weight-aligned" and "weight-mis-aligned" respectively. Also note that $\text{sgn}(w_i)\mathbb{E}\Delta w_i < 0$ signifies that the expected update of weight w_i *shrinks* it toward zero. Conversely, $\text{sgn}(w_i)\mathbb{E}\Delta w_i > 0$ signifies an *expansion* of the weight in the current direction.

- (1). *Weights grow in the right direction starting from zero.* Property 1 of Theorem 3.1 implies that for any $\varepsilon \geq 0$ (i.e. for natural as well as adversarial training) if a feature x_i has weight $w_i = 0$, the SGD update will on average "grow" its weight in the "correct" direction, i.e. in the same direction as its bias b_i , and the expected magnitude of the update is $2|b_i|\bar{\sigma}_i(1)$.
- (2). *Mis-aligned weights are shrunk.* When $\text{sgn}(w_i)\text{sgn}(b_i) = -1$, the upper bound (18) in Property 2 of Theorem 3.1 simplifies to

$$\text{sgn}(w_i)\mathbb{E}\Delta w_i \leq -\bar{\sigma}_i(1)(2|b_i| + \varepsilon),$$

which shows that if the weight of a feature x_i is mis-aligned, then its weight is shrunk toward zero on average, and the magnitude of the shrinkage is proportional to $2|b_i| + \varepsilon$. This makes it clear that adversarial training with a positive value of ε shrinks mis-aligned weights more aggressively than natural training (i.e. with $\varepsilon = 0$), and this effect is even more pronounced for features with large absolute label-correlations.

- (3). *Aligned weights are shrunk by a sufficiently large ε .* When $\text{sgn}(w_i)\text{sgn}(b_i) > 0$, the upper bound (18) simplifies to

$$\text{sgn}(w_i)\mathbb{E}\Delta w_i \leq \bar{\sigma}_i(1)(2|b_i| - \varepsilon), \quad (20)$$

which means that for a weight-aligned feature x_i with bias b_i , if the adversarial ε exceeds the feature's absolute label-correlation $2|b_i|$, then its weight is shrunk toward zero in expectation, and the expected magnitude of the shrinkage is proportional to $\varepsilon - 2|b_i|$.

- (4). *Aligned weights are expanded up to a point, for sufficiently small ε .* When $\text{sgn}(w_i)\text{sgn}(b_i) = 1$, the lower bound (19) simplifies to

$$\text{sgn}(w_i)\mathbb{E}\Delta w_i \geq \bar{\sigma}_i(1) [2|b_i| - |w_i| - \varepsilon(1 + |w_i|)],$$

and this lower bound is positive if $|w_i| < 2|b_i|$ and

$$\varepsilon < \frac{2|b_i| - |w_i|}{1 + |w_i|} \quad (21)$$

In other words, if x_i is weight-aligned, and ε is *sufficiently* smaller than its absolute label-correlation $2|b_i|$ (to account for the $|w_i|$ term in Eq. (21)), then its weight is expanded or preserved on average.

Implications (3) and (4) are specific to adversarial training since they apply only for a certain range of non-zero values of ε . Indeed, these two implications are key to the *feature-concentration* effect of adversarial training which we explore in detail in the experiment sections. Suppose for example that there are two features x_1, x_2 (in the BCP-generated data) with biases $b_1 = 0.2$, and $b_2 = 0.001$ respectively, and we adversarially train a logistic model with $\varepsilon = 0.1$. Then by implication (2) a

negative weight on either feature will be shrunk toward zero on average. Implication (3) means that a positive weight on the "weakly biased" feature x_2 will be shrunk toward zero with a magnitude proportional to almost 0.1. Implication (4) means that a positive weight say $w_1 = 0.05$ on the "strongly biased" feature x_1 will be preserved or expanded since $0.05 < 2b_1 = 0.4$, and $\varepsilon = 0.1$ can be verified to satisfy the bound (21).

More generally, if there are truly random non-predictive features in a data-set, that just happen to show spurious correlations with the label in a finite sample, these features will have much weaker biases than the truly predictive features, and so adversarial training with an appropriate ε would tend to weed out the non-predictive features. We see this phenomenon clearly in the synthetic datasets in the next section, where we intentionally construct a dataset with a mix of predictive and non-predictive random features. In the experiments on the UCI datasets (Section C) and on real-world advertising datasets (Section 6.2) we also see this feature-pruning effect. In these non-synthetic experiments, it is possible that the features being pruned are either truly non-predictive ones, or very weakly biased ones. In datasets with hundreds of thousands of sparse categorical features, pruning even weakly predictive features can be valuable due to the explainability and model-size compression benefits.

Finally, implications (3) and (4) above hint at the possibility of a *goldilocks zone* of ε values which are large enough to weed out irrelevant or weakly-relevant features (i.e. those with tiny biases) and yet small enough to preserve the truly predictive features (i.e. those with significant biases), thus maintaining model performance. For instance if the ordered sequence of absolute feature-label correlations $2|b_i|$ has a *gap* that separates "relevant" features from "irrelevant" or "weakly relevant", then any ε that happens to be in this gap will induce the following behaviors. Eq. (20) suggests that this ε would be *large enough* that it exceeds the absolute label-correlations of the weakly-relevant features, and so their weights will tend to *shrink* even if the features are weight-aligned (and if they are not, then their weights would tend to shrink anyway due to implication (2)). On the other hand Eq. (21) suggests that if the ε is *sufficiently below* the lowest absolute label-correlation of the "relevant" features (to account for the $|w_i|$ term in the bound in Eq. (21)), then the weights of the relevant features are *preserved or expanded*. In other words, adversarial training with an appropriate ε acts as an aggressive *correlation-based feature-filter*, or what we referred to as a *relevance-filter* in Section 1.

The fact that the model-concentration behavior of $\ell_\infty(\varepsilon)$ -adversarial training is realized over a *range* of ε is important from a practical perspective: it implies that we can find a suitable ε more easily and that the desired behavior does not just occur for one "lucky" value.

In case there are a large number of features which are irrelevant or weakly-relevant, then the results of Theorem 3.1 suggest that $\ell_\infty(\varepsilon)$ -adversarial training with an appropriate choice of ε can aggressively weed out the weights of these features, and produce a model which has significantly better *feature-concentration* compared to a naturally-trained one (i.e. with $\varepsilon = 0$).

It should be pointed out that in Theorem 3.1 we do not analyze how adversarial training impacts model accuracy, and we leave this as an open question for future research.

4 Experiments on Synthetic Datasets

The results of Theorem 3.1 and the discussion in Section 3.3 imply that $\ell_\infty(\varepsilon)$ -adversarial training can be perform aggressive *relevance-filtering* when learning a logistic regression model, but the results only apply to data points drawn from the BCP, and only characterize the *expectation* of SGD weight updates. Nevertheless, these results prompt us to ask: Is it possible to reproduce the relevance-filtering behavior of $\ell_\infty(\varepsilon)$ adversarial training on a finite synthetic dataset with a mix of predictive and non-predictive features, without sacrificing standard accuracy? Specifically, we want to design a synthetic dataset where:

- Natural training places non-negligible weights on the predictive features, and on *at least some non-predictive ones*.
- $\ell_\infty(\varepsilon)$ -adversarial training with some $\varepsilon > 0$ places significant weight on the predictive features, but *negligible* weights on the non-predictive features.
- $\ell_\infty(\varepsilon)$ -adversarial training achieves accuracy (or AUC-ROC) comparable to that of natural training, on natural test data.

It turns out that the following synthetic dataset demonstrates the above phenomena very well.

4.1 Synthetic Data Generation and Training Process

The label y is -1 or $+1$ with equal probability. The input vector $x \in \mathbb{R}^d$ consists of 2 kinds of features:

Correlated, strongly predictive features : c identical features $x_1 = x_2 = \dots = x_c$ such that:

$$x_1 = \begin{cases} +y, & \text{w.p. 0.7} \\ -y, & \text{w.p. 0.3} \end{cases} \quad (22)$$

I.I.D, random non-predictive features: r i.i.d. features x_{c+1}, \dots, x_{c+r} each taking the values $+1/-1$ with equal probability.

For our experiments we generate $N = 1000$ data-points according to these specifications, with $c = r = 8$, i.e. 8 identical predictive features and 8 random non-predictive features. The rationale behind these choices of c and r is to ensure that there are "sufficiently many" features of each type, and 8 of each suffices to highlight some of the behaviors we are discussing. The rationale for needing "sufficiently many" is the following: When there are sufficiently many random non-predictive features, some of them will accidentally "look" like they are correlated with the label: this is because in a set of N tosses of a fair coin, the expectation of the fractional imbalance between heads and tails is proportional to $1/\sqrt{N}$, and the distribution of the imbalance is highly concentrated around this expectation. As a result, if there are sufficiently many random non-predictive features, at least some of them will appear correlated with the label, and so natural training will put non-negligible weights on them. Many real-world structured datasets are moderate-sized (say N under a 100,000), and even if the number of data points is very large, there may be a very large number of sparse categorical features, and thus this "spurious" correlation can occur with higher likelihood. When there are several identical, predictive features, natural model training will force these features to "share" their weight roughly equally, thus pushing down the weights to a level comparable or even *less* than that of non-predictive features.

The experimental training and testing methodology is as follows. We train a logistic model (with a non-zero bias term) on the first 700 data-points and test on the remaining 300. For training we use a mini-batch size of 20 and train for 200 epochs, using the FTRL optimizer² with a learning-rate of 0.01, and all weights initialized to zero. During training, we perturb the input vector x using the worst-case $\ell_\infty(\varepsilon)$ adversarial perturbation from Eq. (12) with a specific choice of ε , before taking gradients:

$$\delta_\infty^*(x, y, w, \varepsilon) = -\text{sgn}(w)\varepsilon y \quad (12)$$

4.2 Comparison of Natural and $\ell_\infty(\varepsilon)$ -Adversarial Training with $\varepsilon = 1.0$

Our first experiment is to compare the models resulting from $\ell_\infty(\varepsilon)$ adversarial training with $\varepsilon = 0$ (which is equivalent to natural training), versus $\varepsilon = 1.0$. As shown in Table 1, the AUC and accuracy of the models (on natural test data) are similar, but the learned weights show a dramatic difference. To make it easier to distinguish the random non-predictive features from the predictive features x_1, \dots, x_8 , we relabel the non-predictive features as r_1, \dots, r_8 , and refer to these two feature-groups as "*x*-features" and "*r*-features" respectively. Table 1 shows that after natural training, the ℓ_1 -norm of the predictive features is comparable to that of the non-predictive features, whereas adversarial training reduces the ℓ_1 -norm of the non-predictive features to a negligible amount, while maintaining a significant ℓ_1 -norm on the predictive features.

This contrast between natural and adversarial training is seen clearly in the bar-chart of Figure 1. As expected, natural training results in equal weights on the 8 predictive features (and this is true for adversarial training as well). However natural training also places a significant weight on the 8 random non-predictive features, with 4 of them having *higher* weights than the predictive features. This is clearly problematic from a model-explanation point of view: when explaining the predicted probability on a specific example, we would like to not see the non-relevant features contributing a meaningful amount, and especially not more than the truly predictive features.

²The results are qualitatively similar regardless of which optimizer we use, such as Adam, simple SGD, AdaGrad, etc

training	AUC	accuracy	Wts_x_L1	Wts_r_L1
natural	0.668	0.676	0.724	0.661
adversarial	0.676	0.676	0.205	0.001

Table 1: AUC, Accuracy and model-concentration metrics for natural and $\ell_\infty(\varepsilon)$ adversarial training with $\varepsilon = 1.0$ on the synthetic dataset. The ℓ_1 -norm of the weights of the predictive features is denoted Wts_x_L1, and the ℓ_1 -norm of the weights of the random non-predictive features is denoted Wts_r_L1.

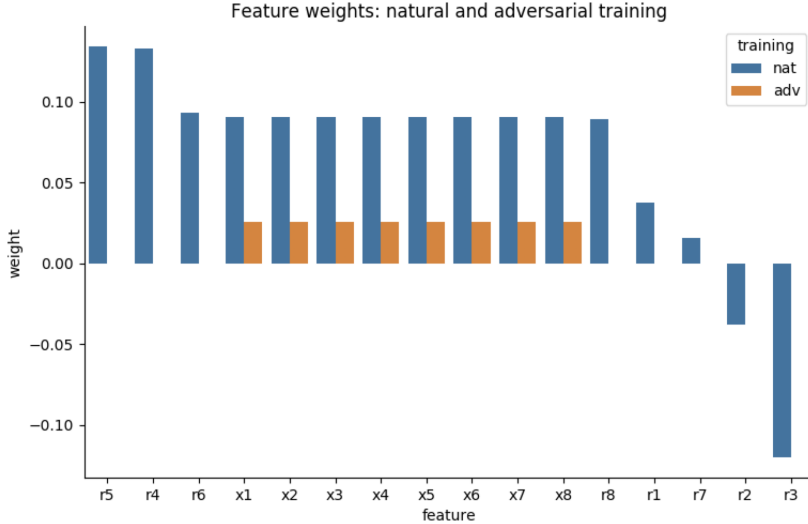


Figure 1: Bar chart of feature weights of logistic model trained on the synthetic dataset with natural training (training = nat, colored grey) and $\ell_\infty(\varepsilon)$ -adversarial training with $\varepsilon = 1.0$ (training = adv, colored orange). The features are shown left to right in decreasing order of absolute value of *naturally-trained* weights. The 8 predictive features are x_1, x_2, \dots, x_8 , and the random non-predictive features x_9, \dots, x_{16} are relabeled r_1, \dots, r_8 to make it easy to distinguish them. Both training modes result in equal weights on the predictive features. However natural training results in all of the non-predictive features having significant weights, with 4 of them having *higher* weights than the predictive features, whereas adversarial training selectively "kills off" all the non-predictive feature-weights, while retaining a significant weight on the predictive ones.

In sharp contrast to natural training, adversarial training does not suffer from this problem: the only significant weights are on the 8 predictive features, and *all* of the non-predictive feature-weights are *selectively killed-off*, with weights close to zero. This is precisely the *aggressive relevance-filtering* effect of adversarial training that we wanted to demonstrate.

4.3 Adversarial Vs Natural Training for a Range of ε values

We gain further insight into the impact of ε on the adversarially-learned model weights, by repeating the above adversarial training (and natural testing) with a range of ε -bounds from 0.0 to 2.0. For each value of ε we separately compute the ℓ_1 -norm of the learned weights of the predictive x -features, and the ℓ_1 -norm of the learned weights of the non-predictive random r -features. These are plotted in Figure 2, along with the AUC on the 300 natural test data points. The figure shows that as ε increases, the ℓ_1 -norm of the weights of the r -features approaches zero much more rapidly than the ℓ_1 -norm of the x -features. Moreover at the level of ε where the r -feature weights approach zero, *the AUC (on natural test data) is nearly as high as the AUC with natural training ($\varepsilon = 0$)*. Notice that there is a range of ε values (shown by the blue band in the figure) which are "just right": i.e. large enough to de-weight non-predictive features, yet small enough to preserve sufficient weight on the predictive features and hence have minimal performance impact on natural test data. This is an instance of the *goldilocks zone* of ε values which we referred to in Section 3.3: $\ell_\infty(\varepsilon)$ -adversarial training with an ε value in this zone yields both *good model explanations* (due to the aggressive relevance-filtering behavior where non-predictive features are given negligible weight) and *good model performance* (since standard accuracy/AUC is maintained).

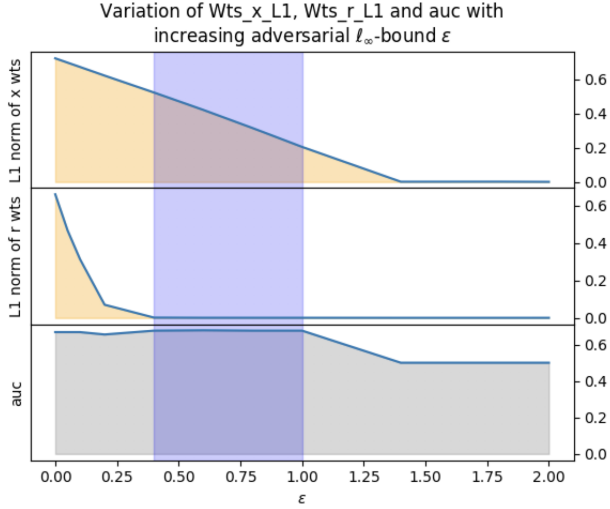


Figure 2: Variation of three quantities in adversarial training as the ε -bound of the ℓ_∞ adversary increases: The top plot shows the ℓ_1 -norm of the predictive x feature-weights. The middle plot shows the ℓ_1 -norm of random non-predictive r feature-weights. The bottom plot shows the AUC on the natural (i.e. unperturbed) test dataset. Note that $\varepsilon = 0$ corresponds to training on natural examples, and as we increase ε , the learned weights of the non-predictive r -features approach zero much more rapidly than those of the predictive x -features, and the ε where the r -weights approach zero still maintains the AUC of a naturally-trained model. The blue band represents the "goldilocks zone" of ε values that are "just right", i.e. adversarial training with this ε bound yields models that have both good explanations (since they eliminate non-predictive features) and good model performance (since AUC is maintained close to the naturally trained level).

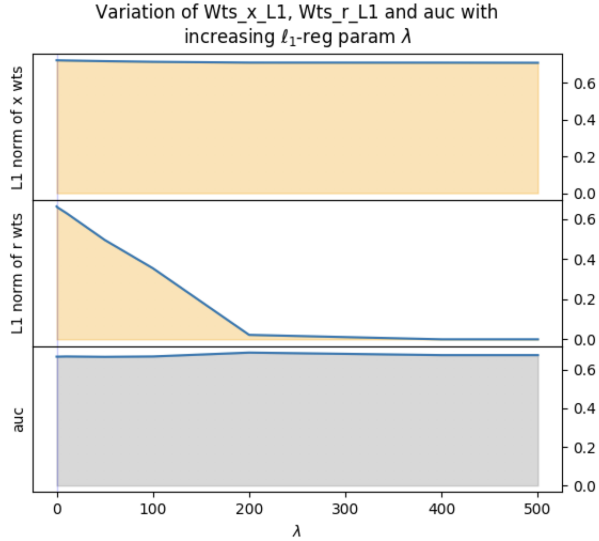


Figure 3: Similar to Figure 2, but keeping ε fixed at 0 (i.e. natural training), and varying the ℓ_1 -regularization parameter λ .

It is natural to wonder whether the feature-weight concentration effect of adversarial training can be achieved using traditional ℓ_1 -regularization. On this specific synthetic dataset we find that indeed it is possible to achieve a similar de-weighting of the non-predictive features using ℓ_1 -regularization with, but this requires a *very large weight* λ on the regularization term in the loss function: it needs to be at least 200, as shown in Figure 3. However as we show in Section 6.2, in large real-world datasets, such a high value of λ damages the AUC of the model considerably, and small λ values do not achieve a model-concentration as significant as that achieved by adversarial training.

4.4 Explanation of Adversarial Training Behavior on the Synthetic Dataset

We can now use Theorem 3.1 to at least partially explain at least some of the observations we made on our synthetic dataset of $N = 1000$ points. Our experiments used a variant of SGD with a mini-batch size of 20 on a shuffled dataset, and so the behavior of the learning algorithm can be reasonably approximated by a modified process where at each stage, a single data-point is drawn uniformly at random with replacement from the N -point dataset and perturbed by the $\ell_\infty(\varepsilon)$ adversary, and presented to the SGD algorithm for a gradient-based update. The random draws of points from the dataset can therefore be modeled as a BCP, with appropriate choices of the biases of each feature. Recall that in the synthetic dataset (Section 4) the 8 *identical* predictive features x_1, x_2, \dots, x_8 each have a bias $b_i = 0.2$, for $i \in [8]$. Since these will share weights equally in the optimal solution, we can reasonably approximate the overall effect of these identical predictive features, using a single feature in the BCP with bias 0.2. The 8 non-predictive features x_9, \dots, x_{16} are each independently uniformly chosen from $\{-1, +1\}$. Thus each non-predictive feature has a probability 0.5 of agreeing or disagreeing with the label y . However in a *finite* sample of N data points, for a non-predictive feature, the expectation of the *fractional absolute imbalance* between agreements and disagreements (with the label) is of the order of $1/\sqrt{N}$, and moreover the distribution of this imbalance is highly concentrated around the expectation. Therefore we can model each of these non-predictive features as a feature in the BCP with an absolute bias of $O(1/\sqrt{N})$.

In other words, we are approximating the synthetic dataset of Section 4 with a BCP where there is one predictive feature with bias 0.2, and 8 features with absolute bias $O(1/\sqrt{N})$. Theorem 3.1 and its implications (Section 3.3) then help us explain the following observations. (It will be helpful to see Figure 1 which shows the weights from natural and adversarial training with $\varepsilon = 1.0$, and Figure 2), which shows the variation of ℓ_1 -norms of the two feature-types with varying ε .)

Observation 1: Natural training (i.e. $\ell_\infty(\varepsilon)$ -adversarial training with $\varepsilon = 0$) places non-negligible weights on at least some of the non-predictive random features, with some of them having weights even larger than predictive features. This is seen in Figure 1. As mentioned before, since the 8 predictive features are identical, natural (and adversarial with any ε) learning results in a model where the weights are shared equally amongst them. On the other hand, many of the random non-predictive features have a bias of $O(1/\sqrt{N})$. Due to implication (1) in Section 3.3, their weights grow from 0 in the direction of their bias, and due to implication (4) they are maintained or expanded in their current direction since $\varepsilon = 0.0$ for natural training. This effect, combined with the fact that the weights of the 8 predictive features are shared equally, causes the weights of some of the non-predictive features to exceed that of the predictive features.

Observation 2: With adversarial training ($\varepsilon = 1.0$) the learned weights on the 8 non-predictive features are close to 0 (Figure 1), but the 8 predictive features retain significant weights. This is the key relevance-filtering effect highlighted by these experiments. Note that $\varepsilon = 1.0$ far exceeds the $O(1/\sqrt{N})$ absolute bias $|b_i|$ of the random-non-predictive features, so by implication (2) in Section 3.3, any mis-aligned weights of these features are shrunk toward zero with an expected change proportional to $\varepsilon + 2|b_i|$, and by implication (3) any aligned weights are also shrunk toward zero, this time with an expected change proportional to $\varepsilon - 2|b_i|$. Both these expected shrinkage rates are close to $\varepsilon = 1$ since the absolute biases $|b_i|$ of these non-predictive features are $O(1/\sqrt{N})$ and therefore negligible compared to 1.0. Note that the single predictive feature has bias 0.2, so by implication (2), if its weight is mis-aligned, it shrinks toward zero with an expected change proportional to $\varepsilon + 2(0.2)$ or 1.4, which is a much more *aggressive* rate than that of the non-predictive features. If the predictive feature has an aligned weight, by implication (3) it shrinks toward zero since $\varepsilon = 1.0 > 2(0.2) = 0.4$, and the expected change is proportional to $\varepsilon - 2(0.2) = 0.6$, which is a much *slower* shrinkage rate than that of the non-predictive features (which is around 1.0). Presumably, after reaching a certain level, the weight of the predictive feature enters the regime of implication (3), which preserves its weight. This can explain why even with $\varepsilon = 1.0$ the weights on the predictive features remain significant.

5 Feature Attribution in 1-Layer Networks

We now turn our attention to measuring feature concentration, which we argue in this paper is a key benefit of $\ell_\infty(\varepsilon)$ -adversarial training on logistic regression models. As mentioned in Section 2.8,

feature concentration could potentially be measured in terms of the model weights, but this is not always the best approach. This is particularly the case for real-world datasets such as those considered in the advertising response prediction task in Section 6.2, where there are many high-cardinality categorical features, and we need an appropriate way to measure an *aggregate* importance of a categorical feature over a dataset. It is therefore worth considering some more principled ways of measuring feature-importance which are amenable to a natural aggregate importance definition.

We find that the feature-attribution method of Integrated Gradients (IG) [2] (described in Section 2.8) is very well suited to our purposes: We derive a *closed-form* expression for the IG-based feature-attributions for a 1-layer neural network (Lemma 5.1), and this makes it computationally very efficient to compute the attributions of all features (which could number into the hundreds of thousands since there are potentially many high-cardinality categorical features). Moreover, in Section 5.2 we propose natural ways to aggregate the IG-based feature-importance metrics across a dataset (which we call Feature Impact and Feature-Value Impact), for categorical as well as numerical features.

5.1 Closed Form for IG in 1-Layer Networks

For general neural networks, the authors of [2] show how to approximate the IG integral (8) by a summation involving gradients at m equally-spaced points along the straight-line path from x' to x . While this approximation is reasonably efficient for a fixed example x and dimension i , it can be prohibitively expensive for computing the IG values across a dataset of millions of examples and thousands of (sparse) features. Closed form expressions for the IG would therefore be of significant interest, especially if the goal is to compute the IG over an entire dataset in order to glean aggregate feature importances.

We first show a closed form exact expression for the $IG_i(x)$ when $F(x)$ is a single-layer network.

Lemma 5.1 (IG Attribution for 1-layer Networks) *If $F(x)$ is computed by a 1-layer neural network (3) with weights vector w , then the Integrated Gradients for all dimensions of x relative to a baseline x' are given by:*

$$IG(x) = [F(x) - F(x')] \frac{(x - x') \odot w}{\langle x - x', w \rangle}, \quad (23)$$

where the \odot operator denotes the entry-wise product of vectors.

Proof: Consider the partial derivative $\partial_i F(x' + \alpha(x - x'))$ in the definition (8) of $IG_i(x)$. For a given x , x' and α , let u denote the vector $x' + \alpha(x - x')$. Then $\partial_i F(u) = \partial F(u)/\partial u_i$, and by applying the chain rule we get:

$$\partial_i F(u) := \frac{\partial F(u)}{\partial u_i} = w_i A'(u),$$

where $A'(u)$ is the gradient of the activation A at u . This implies that:

$$\begin{aligned} \frac{\partial F(u)}{\partial \alpha} &= \sum_{i=1}^d \left(\frac{\partial F(u)}{\partial u_i} \frac{\partial u_i}{\partial \alpha} \right) \\ &= \sum_{i=1}^d [w_i A'(u)(x_i - x'_i)] \\ &= \langle x - x', w \rangle A'(u) \end{aligned}$$

We can therefore write

$$dF(u) = \langle x - x', w \rangle A'(u) d\alpha,$$

and since $\langle x - x', w \rangle$ is a scalar, this yields

$$A'(u) d\alpha = \frac{dF(u)}{\langle x - x', w \rangle}$$

Using this equation the integral in the definition of $IG_i(x)$ can be written as

$$\begin{aligned}
\int_{\alpha=0}^1 \partial_i F(u) d\alpha &= \int_{\alpha=0}^1 w_i A'(u) d\alpha \\
&= \int_{\alpha=0}^1 w_i \frac{dF(u)}{\langle x - x', w \rangle} \\
&= \frac{w_i}{\langle x - x', w \rangle} \int_{\alpha=0}^1 dF(u) \\
&= \frac{w_i}{\langle x - x', w \rangle} [F(x) - F(x')], \tag{24}
\end{aligned}$$

where (24) follows from the fact that $(x - x')$ and w do not depend on α . Therefore from the definition (8) of $IG_i(x)$:

$$IG_i(x) = [F(x) - F(x')] \frac{(x_i - x'_i) w_i}{\langle x - x', w \rangle},$$

and this yields the expression (23) for $IG(x)$. \square

Note that the closed form expression (23) does not depend on the activation derivative A' at all, as long as the activation A is differentiable. There is a natural interpretation of the closed form expression (23): When the input changes from the baseline value x' to x , the dot product changes by $\langle w, x - x' \rangle$, and the fractional contribution of dimension i is $f_i := \frac{w_i(x_i - x'_i)}{\langle w, x - x' \rangle}$, and $IG_i(x)$ is this fraction f_i times the total function value change $F(x) - F(x')$.

5.2 Aggregation of IG Over a Dataset

The IG methodology of [2] only considers feature attribution for a single example x . In order to understand the relative importance of features over a (possibly large) dataset, it would be helpful to somehow aggregate the IG values across multiple examples. We propose here a simple method to do this in structured datasets.

We can now describe our IG aggregation procedure. As mentioned before, we assume that the neural network input is an exploded-form vector x . Note that the i 'th dimension of x corresponds either to a numerical feature in the original feature-vector u , or some specific value of a categorical feature. The IG for each dimension i of x can be computed from Eq. (8) for a general neural network, or from Eq. (23) for a 1-layer network. Informally, $IG_i(x)$ measures the extent to which the i 'th dimension of x contributed to "moving" the network output from its baseline value $F(x')$ to $F(x)$. In other words $IG_i(x)$ represents the *impact* of the i 'th dimension on the output for example x . A reasonable measure of the "importance" of dimension i in some suitable dataset \mathcal{D} is therefore the simple average of $|IG_i(x)|$ over all $x \in \mathcal{D}$. We call this the **feature-value impact** FVI (since the i 'th dimension in exploded space corresponds to a specific value of a categorical feature, or a numeric feature):

$$FVI_i[\mathcal{D}] := \frac{1}{|\mathcal{D}|} \sum_{x \in \mathcal{D}} |IG_i(x)| \tag{25}$$

In the case of a categorical feature, we are also interested in the overall impact of that feature. For example we may want to know what is the overall importance of the `dayOfWeek` feature in some dataset \mathcal{D} . A reasonable way to compute the **feature-impact** FI _{k} , i.e. the overall importance of a categorical feature u_k in original form, is to add the FVI _{i} values over all dimensions i corresponding to this feature in the exploded space:

$$FI_k[\mathcal{D}] := \sum_{i \in I_k} FVI_i[\mathcal{D}] \tag{26}$$

The FI metric is particularly useful to gain an understanding of the aggregate importance of high-cardinality categorical features. For example we measure the feature-concentration of models trained on the MediaMath datasets (which have categorical features with cardinalities in the 100,000 range) in terms of the FI metric (see the FI.L1 and FI.1Pct metrics in Section 6.1).

6 Experiments

In Section 3.2 we analyzed the expectation of the SGD weight-updates of a logistic regression model during $\ell_\infty(\varepsilon)$ -adversarial training, on an *idealized* random data-generation process (the BCP). Theorem 3.1 in that Section suggested that $\ell_\infty(\varepsilon)$ -adversarial training can have an aggressive relevance-filtering (or model-concentration) behavior: the possibility that it aggressively shrinks the weights of irrelevant or weakly-relevant features, while maintaining significant weights on relevant features, and hence not significantly impacting performance on natural test data. In Section 4 we showed that this behavior can be realized on a specific *synthetic* dataset. A natural next question is, whether the model-concentration benefits of $\ell_\infty(\varepsilon)$ -adversarial training can be seen in *real-world* structured datasets. This is the question we explore in this section.

Specifically, we describe the results of experiments intended to answer the following questions for real-world datasets:

1. Is there a "goldilocks zone" of ε values for which significant model-concentration (as measured by various metrics defined in Section 6.1 below) is achieved by $\ell_\infty(\varepsilon)$ -adversarial training, while AUC (on natural test data) is no worse than 0.01 compared to natural training (i.e. with $\varepsilon = 0$) ?
2. Fixing ε at a value in the goldilocks zone, how do the model-weights and IG-based Feature Impact metrics (defined in Section 5.2) in the $\ell_\infty(\varepsilon)$ -adversarially trained model compare with the corresponding metrics in a naturally trained model?
3. If we train the model on natural data, but with ℓ_1 -regularization using a regularization penalty factor λ , can we achieve a similar effect, i.e. produce model-concentration comparable to $\ell_\infty(\varepsilon)$ -adversarial training, and yet maintain AUC within 0.01 of the AUC with $\lambda = 0$?

To answer the above questions, we performed experiments on two kinds of datasets: (a) Two datasets ("mushroom" and "spambase") from the UCI ML data repository [1], and (b) Large-scale real-world ad conversion-prediction datasets from MediaMath. Although the UCI datasets are "real" in the sense that they are derived from real domains, their size has been kept relatively small (typically no larger than a few thousand data records) to facilitate benchmarking, and quick testing or demonstration of ideas. The MediaMath datasets on the other hand have millions of records and hundreds of thousands of (sparse) features, and are actually used to train models that determine bids in the real-time bidding system that the company operates (More details are in Section 6.2).

The findings from our experiments, corresponding to the three questions above, are as follows:

1. For all the datasets studied, there is indeed a "goldilocks zone" of good ε values for which $\ell_\infty(\varepsilon)$ -adversarial training produces significantly more concentrated models with AUC drop (on natural test data) of no more than 0.01 relative to natural training.
2. Examining feature weights or Feature Impact in $\ell_\infty(\varepsilon)$ -adversarially trained models (for a fixed ε in the goldilocks zone) reveals that these models are significantly more concentrated than their naturally-trained counterparts. There are often cases where features given importance by a naturally-trained model are much less important in an $\ell_\infty(\varepsilon)$ -adversarially trained model, and vice versa.
3. On a MediaMath dataset, natural logistic model training with ℓ_1 -regularization using a regularization penalty factor $\lambda = 0.2$ achieves some model concentration but significantly worse than with $\ell_\infty(\varepsilon)$ -adversarial training, and as λ is increased beyond 0.2, the AUC degrades rapidly. A similar effect is seen on the UCI datasets: as λ is increased, the model concentration improves and AUC (on natural test data) drops, but at the point where AUC is 0.01 below the AUC for $\lambda = 0$, model concentration is much inferior to that produced by $\ell_\infty(\varepsilon)$ -regularization.

Section 6.1 describes model training and evaluation methodology. Section 6.2 describes the results from experiments on the MediaMath datasets, and the results from the UCI datasets are in Appendix C.

6.1 Model Training and Evaluation Methodology

We describe here the common aspects of the training and evaluation methodology for the UCI and MediaMath datasets. Any variations specific to the datasets are described in the respective subsections. All the tasks we consider are *probability prediction* tasks as described in Section 2.1, where the prediction target is a binary +1/-1 variable, with +1 indicating a positive example and -1 indicating a negative example. (The specific implementations may actually use a 0/1 label instead, but we keep the -1/1 description here as it simplifies some of the analytical expressions). Our code is implemented in Python using the high-level TensorFlow Estimators and Dataset APIs.

It is important to note that all categorical variables are 1-hot encoded (as described in Section 2.2) prior to being fed to the model-training and evaluation code. In other words we apply the $\ell_\infty(\varepsilon)$ -adversarial perturbation (given by (12)) to the input vector x in *exploded* form. A reasonable question is whether such perturbations are semantically meaningful, and whether they represent legitimate perturbations by an adversary. One could also make the argument that a real adversary would only be able to perturb the original input vector, and so the set of allowed perturbations of x should be restricted to legitimate 1-hot encodings. Indeed some authors have considered this type of restriction in the domain of malware detection [23]. We set aside this issue in this paper, since our interest is more in the model-concentration effect of adversarial training, and less in robustness to real attacks.

Each dataset is divided into train and test subsets. For training on natural examples we use the FTRL optimizer in TensorFlow with ℓ_1 -regularization strength (λ) set to 0. (We vary the λ to evaluate the effect of ℓ_1 -regularization). Our results are substantially the same regardless of which optimizer we use, e.g. Adam, AdaGrad or simple SGD. We use FTRL mainly because in TensorFlow the FTRL optimizer has an optional λ argument that controls the strength of ℓ_1 -regularization. All model weights are initialized to zero in case of the synthetic and toy UCI datasets, whereas they are initialized using a Gaussian initializer (with mean 0 and variance 0.001) in the case of the MediaMath ad response-prediction models. Once again our results remain the same whether we use zero or Gaussian initializers. For $\ell_\infty(\varepsilon)$ -adversarial training we also use the FTRL optimizer, except that in each mini-batch the examples x are perturbed according to the worst-case perturbation given by Eq. 12, as described in the canonical SGD setup in Section 2.6. Some authors train adversarially robust models by first training on natural examples and then training on adversarial examples. But in our experiments we find that the initial pre-training on natural examples does not make a difference, at least for the model-concentration effects which we are studying.

Once a model is trained (adversarially or naturally) we compute two types of metrics:

- An *ML performance* metric, the AUC-ROC (Area Under the ROC Curve) on the held-out *natural test dataset*.
- A few *feature concentration* metrics, defined as follows, where the linear model weight-vector is $w \in \mathbb{R}^d$ (and d is the dimension of the *exploded* feature-space, i.e. after 1-hot encoding).

Wts.L1: $\|w\|_1/\|w\|_\infty$, which is a measure of the overall magnitude of the weights, scaled by the biggest absolute weight. Note that if we multiply all weights by a constant factor, then WtsL1 does not change.

Wts.1Pct: The percent of the weights in w whose absolute value is at least 1% of the maximum absolute weight. This can be thought of as a measure of how many feature-weights are "significant", where the threshold of significance is 1% of the biggest absolute weight.

FI.L1: $\|FI\|_1/\|FI\|_\infty$, where FI stands for the vector of Feature Impact values $FI_i[\mathcal{D}]$ (defined by Eq (26)), and i ranges over the dimensions in the *original* feature-space (i.e. before 1-hot encoding), and the dataset \mathcal{D} is the *natural training dataset*.

FI.1Pct: The percent of components of FI (which are all positive by definition) that are at least 1% of the biggest component of FI , again over the natural training dataset.

In all our experiments, when we use the closed-form formula in Eq. (23) to compute the FVI (Feature-Value Impact) values (Eq (25)) of the dimensions of the exploded feature-vector, for the baseline input x' we use the all-zeros vector.

In the various tables of results, we use the abbreviation `nat` to refer to metrics for the naturally-trained model, and `adv` to refer to metrics for the adversarially-trained model.

6.2 Experiments with MediaMath Datasets: Ad Conversion Prediction

MediaMath provides a software platform that operates a real-time bidding (RTB) engine which responds to bid-opportunities sent by ad-exchanges. The RTB engine bids on behalf of advertisers who set up ad-campaigns on the platform. A key component in determining bid prices is a prediction of the probability that a consumer exposed to the advertiser's campaign would subsequently perform a certain designated action (called a "conversion"). MediaMath currently trains a logistic regression model for each campaign to generate these conversion probability predictions. The models are trained on a dataset collected over a number of days, where each record contains various features related to the ad opportunity (such as device type, browser, location, time of day etc), as well as a 0/1 label indicating whether or not a conversion occurred subsequent to ad exposure. The model for each campaign is trained on a sequence of 18 days of data, and validated/tested on the subsequent 3 days of data. The total number of records in each dataset can range from half million to 50 million depending on the campaign. Each record has around 100 features, mostly categorical, and some (such as "siteID") have cardinalities as high as 100,000, and so the dimension of the exploded feature-space (i.e. after 1-hot encoding) is on the order of 400,000. (We use feature-hashing rather than explicit 1-hot encoding to map some of the high-cardinality features to a lower-dimensional vector, but the net effect is similar to 1-hot encoding, except that now each dimension in the 1-hot encoding vector may correspond to multiple features, due to hash collisions)

Given the extremely high dimensionality of the exploded feature-space, it is of considerable practical importance to understand which features have a truly significant impact on the predictions. Specifically, we wish to explore whether adversarial training can yield models that have significantly better feature concentration, while maintaining the AUC within say 0.01 of the naturally-trained model. We have seen strong evidence that this is indeed possible, both on synthetic datasets (Section 4) and on some UCI datasets (Section C). We show below that we see a similar phenomenon in the conversion-prediction models.

To study the impact of $\ell_\infty(\varepsilon)$ adversarial training, we performed experiments with a wide range of values of ε and found that for most campaigns, adversarial training with $\varepsilon = 0.01$ or $\varepsilon = 0.001$ results in feature-concentrations significantly better than with natural training, while maintaining AUC (on the validation set) within 0.01 of the AUC of a naturally-trained model. We also experimented with keeping $\varepsilon = 0$ and varying the ℓ_1 -regularization parameter λ in the FTRL optimizer, and found that any $\lambda > 0.2$ significantly lowers the AUC of the resulting model, and lower λ values do not yield a feature-concentration as strong as that achieved by adversarial training. Indeed we find that the effects of adversarial training and ℓ_1 regularization are complementary: when an appropriate value of ε is used in conjunction with say $\lambda = 0.01$, we find that ℓ_1 regularization helps to "clean" up the very low feature-weights produced by adversarial training by pushing them to zero.

Table 2 shows a summary of results on 9 campaigns³. In some cases the AUC of the adversarially-trained model is better than that of the naturally-trained model. Recall that the Wts.1Pct metric measures what percent of dimensions (in the exploded space, after 1-hot encoding) have absolute weights at least 1 percent of the highest absolute weight. Since most features are categorical, Wts.1Pct is therefore a measure of what percent of *feature-values* are significant to the model. This metric (as well as Wts.L1) falls drastically with adversarial training in all cases, which indicates that several of the feature-values are simply not relevant to predicting the label. There is thus a potentially massive *model-compression* that can be done, and this can have benefits in storing, updating and serving models (MediaMath periodically trains around 40,000 models). Table 2 also shows the FI.1Pct and FI.L1 metrics, which are aggregate feature-impact concentration metrics over the natural training dataset. Note that these are at the *feature* level and not feature-value level. Since the FI measure of a categorical feature aggregates the FVI metric over all values of this feature, the drop in this metric (when we go from natural to adversarial training) is not as dramatic as in the case of Wts.L1 or Wts.1Pct (and sometimes these are higher than with natural training).

³All campaign IDs and feature names are masked for client confidentiality reasons

Campaign	training	AUC	Wts.1Pct	Wts.L1	FI.1Pct	FI.L1
285	nat	0.560	12.93	165.05	0.78	5.80
	adv ($\varepsilon = 0.01$)	0.556	0.39	13.27	0.37	2.87
479	nat	0.697	11.23	92.02	3.20	12.52
	adv ($\varepsilon = 0.001$)	0.694	6.17	66.96	3.13	12.34
622	nat	0.565	27.11	110.12	6.63	5.73
	adv ($\varepsilon = 0.01$)	0.561	4.21	18.18	2.87	3.55
594	nat	0.702	16.91	172.55	0.86	12.54
	adv ($\varepsilon = 0.001$)	0.702	1.09	19.97	0.77	11.19
473	nat	0.683	28.02	177.36	3.14	14.69
	adv ($\varepsilon = 0.001$)	0.673	3.58	55.68	2.84	15.69
070	nat	0.622	18.53	158.15	4.94	26.21
	adv ($\varepsilon = 0.001$)	0.625	7.55	107.63	4.46	24.00
645	nat	0.573	16.26	251.37	2.78	31.78
	adv ($\varepsilon = 0.01$)	0.627	1.07	34.45	1.12	10.60
733	nat	0.658	27.35	203.73	4.04	11.36
	adv ($\varepsilon = 0.001$)	0.667	9.91	108.03	4.13	11.60
735	nat	0.758	12.20	220.97	1.87	21.82
	adv ($\varepsilon = 0.01$)	0.765	0.51	21.02	0.75	16.36

Table 2: Comparison of AUC and feature-concentration between natural and adversarial training on 9 advertising campaigns. The 4 concentration metrics are defined in Section 6.1. Note that while the AUC is computed on the natural validation set, the concentration metrics FI.1Pct and FI.L1 are computed on the natural training dataset. In some campaigns, such as 285, 735 the Wts.1Pct metric improves by a factor of more than 24.

To illustrate the effect of adversarial training in more detail, we focus on campaign number 735 (the bottom row in Table 2) and compare the results from natural training and adversarial training (with $\varepsilon = 0.01$). Figure 4 compares the Feature Impact (FI) values between these models; Figure 5 compares the feature-weights drop-off curves of these models; and Figure 6 compares the FI drop-off curves.

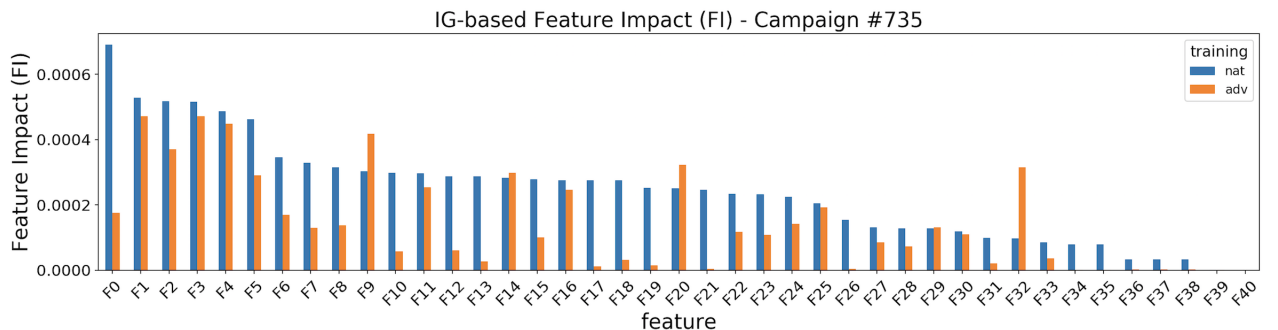


Figure 4: Comparison of aggregate Feature Impact (FI defined in Eq. (26)) for a naturally-trained model, and an adversarially-trained model with $\varepsilon = 0.01$, on the dataset for Campaign 735. The features are arranged left to right in decreasing order of their FI in the naturally-trained model.

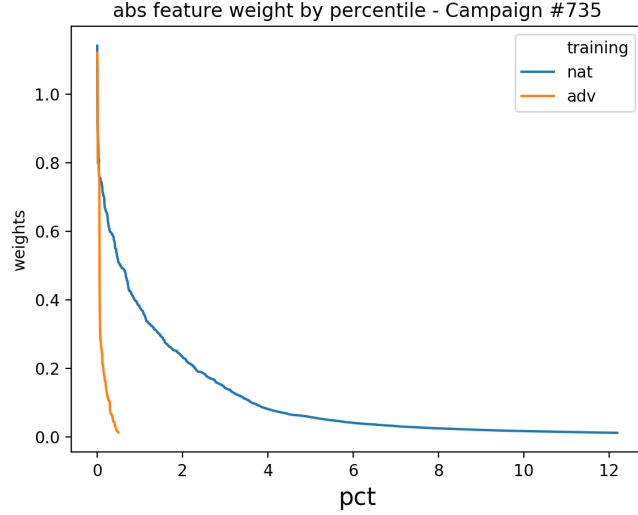


Figure 5: Comparison of drop-off of absolute feature weights in natural and adversarial training (with $\varepsilon = 0.01$), for Campaign 735. In each curve the y -coordinate of the point corresponding to a percent p equals the weight of the feature at the p 'th percentile when the weights are arranged in decreasing absolute value. Each curve is truncated when the weight reaches 1% of the highest weight in the respective model. The adversarially trained model has a much steeper weight drop-off, with only 0.5% being above the 1% threshold, compared to 12% with natural training (this is consistent with Table 2).

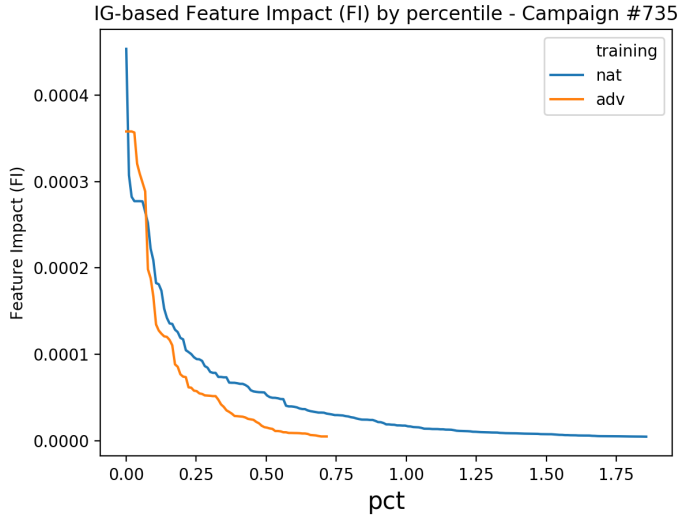


Figure 6: Comparison of drop-off of aggregate Feature Impact (FI) (computed over the natural training dataset) for a naturally-trained and adversarially-trained model (with $\varepsilon = 0.01$), for Campaign 735. In each curve the y -coordinate of the point corresponding to a percent p equals the weight of the feature at the p 'th percentile when the weights are arranged in decreasing absolute value. Each curve is truncated when the FI reaches 1% of the highest FI in the respective model. The adversarially trained model has a much steeper FI drop-off, with only 0.75% being above the 1% threshold, compared to 1.87% with natural training. (this is consistent with Table 2).

Figures 7 and 8 contrast the ability of adversarial training and ℓ_1 regularization to improve model concentration while maintaining AUC (on natural test data): adversarial training with $\varepsilon=0.01$ improves the concentration metric Wts.1Pct to as low as 0.5% (compared to 12% for a naturally trained model, an improvement factor as high as 24), and yet achieves an AUC slightly higher than with natural training. On the other hand with ℓ_1 regularization, using a strength of $\lambda = 0.2$ improves the

concentration to 5% (significantly worse than 0.5% for adversarial training) and slightly improves upon the naturally-trained AUC, but any higher value of λ significantly degrades the AUC, and the Wts.1Pct concentration metric does not go below 2.5%.

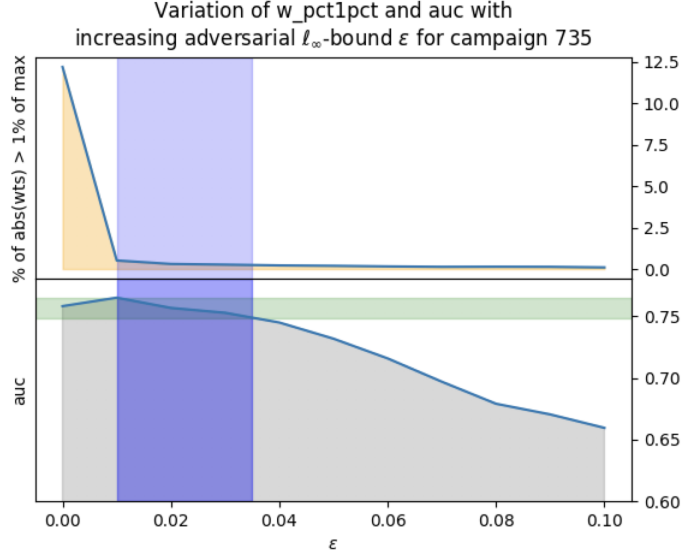


Figure 7: Variation of Wts.1Pct and natural test AUC with increasing ε bound on ℓ_∞ perturbations in adversarial training, for campaign 735. Note that $\varepsilon = 0$ corresponds to natural training, which results in $\text{AUC}=0.758$. The horizontal green band lower-bounded by $\text{AUC}=0.748$ represents the range of AUCs within 0.01 of AUC of the naturally-trained mode. The blue vertical band represents the range of ε values (0.01 to 0.03) that are high enough to produce significant model-concentration (i.e. reduction in Wts.1Pct), yet low enough that AUC is maintained within the green band. For these values of ε , the Wts.1Pct metric is under 0.5%, meaning that only 0.5% of absolute weights are within 1% of the highest absolute weight.

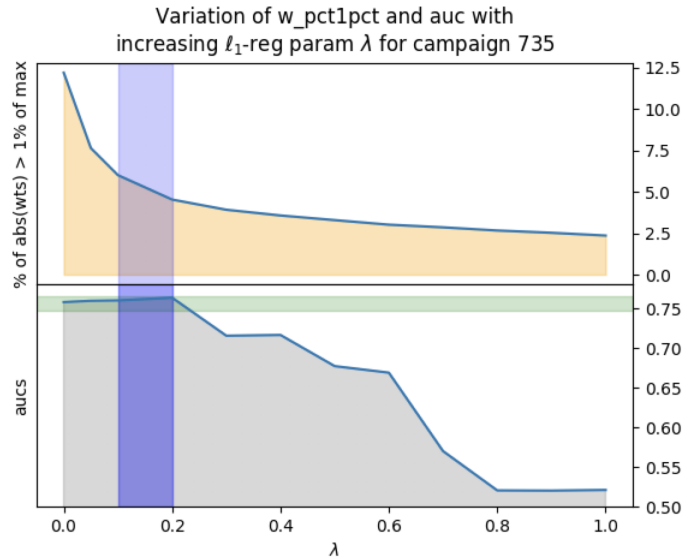


Figure 8: Variation of Wts.1Pct and natural test AUC for naturally-trained models, with increasing ℓ_1 -regularization parameter λ , for campaign 735. For a $\lambda = 0.2$, the Wts.1Pct concentration metric is as high as 5% (significantly worse than the 0.5% for adversarial training), and any higher value of λ significantly degrades the AUC.

7 Conclusion and Future Work

We considered the question of whether adversarial learning can be used as a mechanism to trim logistic models significantly, while maintaining performance (as measured by AUC or accuracy) on natural (unperturbed) test data. From an explainability standpoint, it is highly desirable that models do not heavily weigh features that are irrelevant or marginally influential. We explored this possibility of feature-concentration both theoretically and empirically, in the context of logistic regression models and ℓ_∞ -bounded adversaries. On the theory side, we derived results showing bounds on the expectation of the weight updates, in terms of the adversarial ε bound, the feature's bias, its current weight, and the current overall learning stage of the model. Our results suggest there is often a *goldilocks zone* of adversarial ε bounds that are "just right": large enough to weed out irrelevant features, yet small enough to maintain reasonable weights on truly predictive ones and hence not impact model performance on natural test data. The practical implication of the goldilocks zone is that it makes it easy to find a suitable ε , so the desired behavior is restricted to just one (or a few) "lucky" value of ε .

Our theory both motivates and at least partially explains our experimental studies. We designed a synthetic dataset containing a mix of predictive features and random non-predictive features, and showed that natural learning tends to learn significant weights on the non-predictive features (some of which are higher than that of the predictive features) simply because they show spurious correlations with the label in a finite sample of data. By contrast adversarial training with a large enough ε bound can weed out these noise features while maintaining weights on the predictive features, hence minimally impacting (if at all) the model's performance on natural test data.

We demonstrate the feature-pruning effect of adversarial training on two toy UCI datasets and real-world advertising response-prediction datasets from MediaMath. On the latter datasets we showed that adversarial training with ℓ_∞ perturbations with ε bounds as small as 0.001 or 0.01 can achieve as much as a factor of 20 reduction in the number of "significant" weights (defined as the number of weights whose magnitudes are within 1% of the maximum magnitude), and yet their performance on natural test data is not impacted, and sometimes even improves upon natural training.

We also showed that this effect is not easily replicated with ℓ_1 -regularization. In particular we showed that in the synthetic datasets, one needs to use an unusually-large value of the regularization-weight λ whereas there is no λ that achieves a comparable effect in the UCI datasets and real-world MediaMath datasets.

It is worth pointing out that on *specific* datasets, it may well be possible to reproduce this model-concentration behavior with natural model training, using *carefully custom-designed* hyper-parameters (such as a learning-rate schedule customized to the dataset). We emphasize, however, that it is *simpler* to achieve this behavior using $\ell_\infty(\varepsilon)$ -adversarial training: it merely involves trying a set of ε values, without the need for specially customizing the other hyper-parameters.

To speed up adversarial training we relied on our closed-form formula for the worst-case adversarial perturbation for logistic models. We quantified feature-concentration in a few different ways, including some that are based on the model weights, and some derived from the Integrated-Gradient (IG) based feature-attribution method. We derived a closed-form formula for the IG-based feature-attribution, for 1-layer neural networks, which we leverage to be able to compute a new metric of aggregate feature importance we introduced, called Feature Impact.

It would be of significant interest to expand our theoretical analysis of adversarial learning, and in particular show a link to accuracy (which is something we did not do, unlike the analysis of [6]). Also, a nice result would be to precisely show why ℓ_1 regularization does not achieve a feature-pruning effect comparable to adversarial learning. Deriving closed form formulas (or efficient approximations) for adversarial perturbations, as well as feature-attributions, for more complex networks would also help make adversarial training and measurement of aggregate feature impact more practical.

Another direction for exploration is to consider more carefully the notion of an adversarial perturbation in structured datasets (a point that was alluded to at the beginning of Section 6). In image domains, an adversarial perturbation is one that preserves perceptual similarity (from a human observer's perspective) and yet causes a model to misclassify the example. We have side-stepped this issue in this paper since our primary motivation was to study the model-concentration effects of adversarial learning. However even for this specific purpose, it may be useful to consider other classes of

permissible perturbations, such as perturbations that are constrained to be valid inputs when the features are categorical (for example [23] consider this type of restriction for adversarially robust detection malware detection). In our experiments, we perturb the 1-hot encoded vector along all dimensions, which will in general result in a vector that is not a valid representation of any input vector (since multiple dimensions corresponding to a single categorical feature may be non-zero). It is possible that such constrained perturbations produce even better results from a model-concentration point of view.

References

- [1] D. Dheeru and E. Karra Taniskidou, “UCI machine learning repository,” 2017. <http://archive.ics.uci.edu/ml>.
- [2] M. Sundararajan, A. Taly, and Q. Yan, “Axiomatic attribution for deep networks,” *arXiv:1703.01365 [cs.LG]*.
- [3] C. Szegedy, W. Zaremba, I. Sutskever, J. Bruna, D. Erhan, I. Goodfellow, and R. Fergus, “Intriguing properties of neural networks,” *arXiv:1312.6199 [cs.CV]*. <http://arxiv.org/abs/1312.6199>.
- [4] I. J. Goodfellow, J. Shlens, and C. Szegedy, “Explaining and harnessing adversarial examples,” *arXiv:1412.6572 [stat.ML]*. <http://arxiv.org/abs/1412.6572>.
- [5] N. Papernot, P. McDaniel, S. Jha, M. Fredrikson, Z. Berkay Celik, and A. Swami, “The limitations of deep learning in adversarial settings,” *arXiv:1511.07528 [cs.CR]*. <http://arxiv.org/abs/1511.07528>.
- [6] A. Madry, A. Makelov, L. Schmidt, D. Tsipras, and A. Vladu, “Towards deep learning models resistant to adversarial attacks,” *arXiv:1706.06083 [stat.ML]*.
- [7] A. Sinha, H. Namkoong, and J. Duchi, “Certifying some distributional robustness with principled adversarial training,” Feb., 2018.
- [8] K. Leino, L. Li, S. Sen, A. Datta, and M. Fredrikson, “Influence-Directed explanations for deep convolutional networks,” *arXiv:1802.03788 [cs.LG]*. <http://arxiv.org/abs/1802.03788>.
- [9] M. Ancona, E. Ceolini, C. Öztireli, and M. Gross, “Towards better understanding of gradient-based attribution methods for deep neural networks,” *arXiv:1711.06104 [cs.LG]*. <http://arxiv.org/abs/1711.06104>.
- [10] R. Guidotti, A. Monreale, S. Ruggieri, F. Turini, D. Pedreschi, and F. Giannotti, “A survey of methods for explaining black box models,” *arXiv:1802.01933 [cs.CY]*. <http://arxiv.org/abs/1802.01933>.
- [11] G. Ras, M. van Gerven, and P. Haselager, “Explanation methods in deep learning: Users, values, concerns and challenges,” *arXiv:1803.07517 [cs.AI]*. <http://arxiv.org/abs/1803.07517>.
- [12] A. Kurakin, I. Goodfellow, and S. Bengio, “Adversarial machine learning at scale,” *arXiv:1611.01236 [cs.CV]*. <http://arxiv.org/abs/1611.01236>.
- [13] D. Tsipras, S. Santurkar, L. Engstrom, A. Turner, and A. Madry, “Robustness may be at odds with accuracy,” *arXiv:1805.12152 [stat.ML]*. <http://arxiv.org/abs/1805.12152>.
- [14] H. Kannan, A. Kurakin, and I. Goodfellow, “Adversarial logit pairing,” *arXiv:1803.06373 [cs.LG]*. <http://arxiv.org/abs/1803.06373>.
- [15] D. Tsipras, S. Santurkar, L. Engstrom, A. Turner, and A. Madry, “There is no free lunch in adversarial robustness (but there are unexpected benefits),” *arXiv:1805.12152 [stat.ML]*.
- [16] L. Schmidt, S. Santurkar, D. Tsipras, K. Talwar, and A. Mądry, “Adversarially robust generalization requires more data,” *arXiv:1804.11285 [cs.LG]*. <http://arxiv.org/abs/1804.11285>.
- [17] H. Brendan McMahan, G. Holt, D. Sculley, M. Young, D. Ebner, J. Grady, L. Nie, T. Phillips, E. Davydov, D. Golovin, S. Chikkerur, D. Liu, M. Wattenberg, A. M. Hrafnkelsson, T. Boulos, and J. Kubica, “Ad click prediction: a view from the trenches,”. <https://ai.google/research/pubs/pub41159>.
- [18] O. Chapelle, E. Manavoglu, and R. Rosales, “Simple and scalable response prediction for display advertising,” *ACM Trans. Intell. Syst. Technol.* **5** no. 4, (Dec., 2014) 61:1–61:34. <http://doi.acm.org/10.1145/2532128>.

- [19] J. Zhao, A. Henriksson, L. Asker, and H. Boström, “Predictive modeling of structured electronic health records for adverse drug event detection,” *BMC Med. Inform. Decis. Mak.* **15 Suppl 4** (Nov., 2015) S1. <http://dx.doi.org/10.1186/1472-6947-15-S4-S1>.
- [20] P. McCullagh and J. Nelder, *Generalized Linear Models, Second Edition*. Chapman and Hall/CRC Monographs on Statistics and Applied Probability Series. Chapman & Hall, 1989. http://books.google.com/books?id=h9kFH2_FfBkC.
- [21] X. Yuan, P. He, Q. Zhu, and X. Li, “Adversarial examples: Attacks and defenses for deep learning,” [arXiv:1712.07107 \[cs.LG\]](https://arxiv.org/abs/1712.07107). <http://arxiv.org/abs/1712.07107>.
- [22] T. Fawcett, “An introduction to ROC analysis,” *Pattern Recognit. Lett.* **27** no. 8, (June, 2006) 861–874. <http://www.sciencedirect.com/science/article/pii/S016786550500303X>.
- [23] A. Al-Dujaili, A. Huang, E. Hemberg, and U.-M. O'Reilly, “Adversarial deep learning for robust detection of binary encoded malware,” [arXiv:1801.02950 \[cs.CR\]](https://arxiv.org/abs/1801.02950).

Appendix A Proof of proposition 3.1

Proposition 3.1 (Gradient of Logistic NLL Loss under $\ell_\infty(\varepsilon)$ adversarial perturbation) *If L is the logistic NLL loss given by (5), and $x' = x + \delta^*$ where δ^* is the $\ell_\infty(\varepsilon)$ adversarial perturbation (12), then for each $i \in [d]$ the gradient $\partial L(x', y; w)/\partial w_i$ is given by:*

$$\frac{\partial L(x', y; w)}{\partial w_i} = -\sigma(\varepsilon\|w\|_1 - y\langle x, w \rangle)(yx_i - \varepsilon \operatorname{sgn}(w_i)) \quad (13)$$

Proof: Consider first the logistic NLL loss in Eq. (5). If we write z for the dot product $\langle w, x \rangle$, the loss can be written as $L = \ln(1 + e^{-yz}) = -\ln(\sigma(yz))$ where σ is the sigmoid function. Then the gradient $\partial L/\partial w_i$ is given by:

$$\begin{aligned} \frac{\partial L}{\partial w_i} &= \frac{\partial L}{\partial z} \frac{\partial z}{\partial w_i} \\ &= -\frac{\sigma'(yz)}{\sigma(yz)} yx_i \\ &= -\sigma(-yz)yx_i \\ &= -\sigma(-y\langle x, w \rangle) yx_i, \end{aligned} \quad (27)$$

where σ' stands for the derivative of σ with respect to its argument, and we used the fact that $\sigma'(u) = \sigma(u)\sigma(-u)$. The result then follows from (27) by observing that

$$\begin{aligned} y\langle x', w \rangle &= y\langle x - \varepsilon y \operatorname{sgn}(w), w \rangle \\ &= y\langle x, w \rangle - \varepsilon\|w\|_1, \end{aligned}$$

and

$$yx'_i = yx_i - \varepsilon \operatorname{sgn}(w_i)$$

□

Appendix B Proof of theorem 3.1

The proof relies on two properties of the conditional expectation $\bar{\sigma}_i(s)$ (defined in Eq. 16)), which we state in this Lemma:

Lemma B.1 (Properties of $\bar{\sigma}_i(s)$)

$$\bar{\sigma}_i(1) \leq \bar{\sigma}_i(-1), \quad \text{with equality when } w_i = 0 \quad (28)$$

$$\bar{\sigma}_i(-1) \leq \bar{\sigma}_i(1)(1 + 2|w_i|) \quad (29)$$

Proof: Notice that in the argument of the $\sigma()$ in the expectation (16), the only terms involving feature i are $\varepsilon|w_i| - yx_i w_i$, and in particular the term $-yx_i w_i$ is the only term that is different between $\bar{\sigma}_i(-1)$ and $\bar{\sigma}_i(1)$. Moreover, this term is larger in $\bar{\sigma}_i(-1)$ by an amount $2|w_i|$ than in $\bar{\sigma}_i(1)$. The first property then follows from monotonicity of the sigmoid function, and the second is a consequence of the fact that for any positive h , $\sigma(u + h) \leq \sigma(u)(1 + h)$. □

We are now ready to show the main result characterizing the expected gradient update $\mathbb{E}(\Delta w_i)$ for individual features.

Theorem 3.1 (Expectation of logistic gradient update for the BCP) *Given a weight vector $w \in \mathbb{R}^d$, assuming a learning rate $\eta = 1$ (only to avoid notational clutter), if a data point (x, y) is drawn according to the BCP above, and $x' = x + \delta^*$ where δ^* is the $\ell_\infty(\varepsilon)$ adversarial perturbation given by Eq. (12), then for each $i \in [d]$, the expectation (over random draws from the BCP) of the SGD update Δw_i (defined in Eq. (15)) satisfies the following properties:*

1. If $w_i = 0$ then

$$\mathbb{E}\Delta w_i = 2b_i\bar{\sigma}_i(1) = 2b_i\bar{\sigma}_i(-1). \quad (17)$$

2. If $w_i \neq 0$, then

$$\text{sgn}(w_i)\mathbb{E}\Delta w_i \leq \bar{\sigma}_i(1)(2\text{sgn}(w_i)b_i - \varepsilon) \quad (18)$$

and

$$\text{sgn}(w_i)\mathbb{E}\Delta w_i \geq \bar{\sigma}_i(1)[2b_i\text{sgn}(w_i) - |w_i| - \varepsilon(1 + |w_i|)] \quad (19)$$

Proof: From (15) and (13), since η is assumed to be 1,

$$\Delta w_i = \sigma(\varepsilon\|w\|_1 - y\langle x, w \rangle)(yx_i - \varepsilon\text{sgn}(w_i)) \quad (30)$$

When $w_i = 0$ this simplifies to

$$\Delta w_i = yx_i\sigma(\varepsilon\|w\|_1 - y\langle x, w \rangle),$$

and we can compute the expectation by conditioning on the two possibilities $yx_i \pm 1$, which have respective probabilities $0.5 \pm b_i$ (from the definition of the BCP above). Using the definition (16) of the conditional expectations $\bar{\sigma}_i(1)$ and $\bar{\sigma}_i(-1)$ (which are equal since $w_i = 0$), this expectation can be written as

$$\begin{aligned} \mathbb{E}\Delta w_i &= (0.5 + b_i)\bar{\sigma}_i(1) - (0.5 - b_i)\bar{\sigma}_i(-1) \\ &= 2b_i\bar{\sigma}_i(1), \end{aligned}$$

which establishes Property 1.

Now consider the case $w_i \neq 0$. We want to decompose the expectation $\mathbb{E}\Delta w_i$ by conditioning over two possibilities, $yx_i \text{sgn}(w_i) = \pm 1$. From the definition of the BCP, it can be seen that these possibilities occur with respective probabilities $0.5 \pm b_i \text{sgn}(w_i)$. Also, since $yx_i \text{sgn}(w_i) = \pm 1$ is equivalent to $yx_i = \pm \text{sgn}(w_i)$ respectively, we can write the following

$$\begin{aligned} \mathbb{E}\Delta w_i &= (0.5 + b_i \text{sgn}(w_i))(\text{sgn}(w_i) - \varepsilon \text{sgn}(w_i))\bar{\sigma}_i(1) \\ &\quad - (0.5 - b_i \text{sgn}(w_i))(\text{sgn}(w_i) + \varepsilon \text{sgn}(w_i))\bar{\sigma}_i(-1), \end{aligned} \quad (31)$$

where we use the definition (16) of the conditional expectations $\bar{\sigma}_i(1)$ and $\bar{\sigma}_i(-1)$. Multiplying throughout by $\text{sgn}(w_i)$ yields

$$\begin{aligned} \text{sgn}(w_i)\mathbb{E}\Delta w_i &= (0.5 + b_i \text{sgn}(w_i))(1 - \varepsilon)\bar{\sigma}_i(1) \\ &\quad - (0.5 - b_i \text{sgn}(w_i))(1 + \varepsilon)\bar{\sigma}_i(-1) \\ &\leq (0.5 + b_i \text{sgn}(w_i))(1 - \varepsilon)\bar{\sigma}_i(1) \\ &\quad - (0.5 - b_i \text{sgn}(w_i))(1 + \varepsilon)\bar{\sigma}_i(1) \\ &= (2b_i \text{sgn}(w_i) - \varepsilon)\bar{\sigma}_i(1) \end{aligned} \quad (32)$$

where the inequality (32) is justified by the facts that $\bar{\sigma}_i(-1) \leq \bar{\sigma}_i(1)$ (Lemma B.1), and that the factors in the second term in the first equation are all non-negative. This establishes the upper bound (18).

To argue the lower bound (19), we apply the inequality $\bar{\sigma}_i(-1) \leq \bar{\sigma}_i(1)(1 + 2|w_i|)$ (Lemma B.1) in Eq. (31), which after simplification yields

$$\text{sgn}(w_i)\mathbb{E}\Delta w_i \geq \bar{\sigma}_i(1)[(2b_i \text{sgn}(w_i) - \varepsilon) - (1 - 2b_i \text{sgn}(w_i))(1 + \varepsilon)|w_i|],$$

and this implies the desired lower bound since $1 - 2b_i \text{sgn}(w_i) \leq 1$. \square

Appendix C Experiments on some UCI datasets

We now describe experiments on datasets in the popular UCI repository of ML datasets. We show details of experiments on two of these datasets:

- The **mushroom** dataset consists of 8142 instances, each of which corresponds to a different mushroom species, and has 22 categorical features (and no numerical features), whose cardinalities are all under 10. The task is to classify an instance as edible (label=1) or not (label=0).
- The **spambase** dataset consists of 4601 instances with 57 numerical attributes (and no categorical ones). The instances are various numerical features of a specific email, and the task is classify the email as spam (label = 1) or not (label = 0).

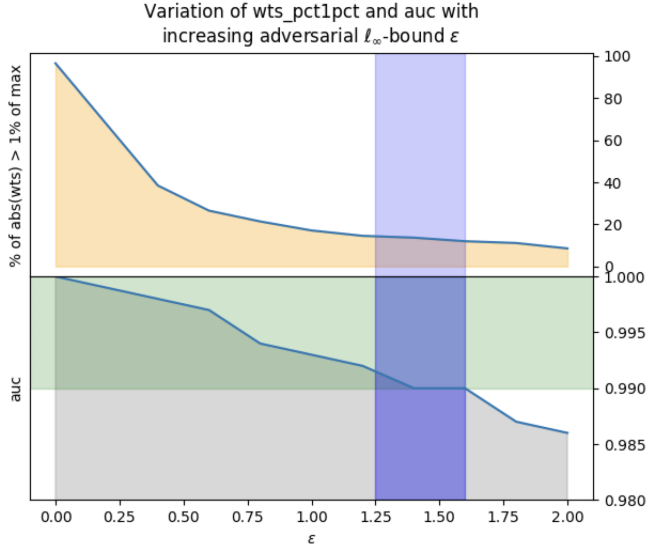


Figure 9: Variation of Wts.1Pct and test AUC with increasing ε bound on ℓ_∞ perturbations in adversarial training, for the mushroom dataset. Note that $\varepsilon = 0$ corresponds to natural training, which results in AUC=1.00. The horizontal green band from AUC=0.99 to AUC=1.00 shows the range of AUCs within 0.01 of AUC of the naturally-trained mode. The blue vertical band represents the goldilocks zone of ε values (roughly 1.25 to 1.6) that are high enough to produce significant model-concentration, yet low enough that AUC is maintained within the green band.

In each case our training and testing methodology is similar to that used on the synthetic datasets: we split the dataset randomly into a 70% training dataset and a 30% test dataset. We train a logistic model using the FTRL optimizer (where the strength λ of ℓ_1 regularization can be adjusted), with all weights initialized to zero. Prior to training and testing, we standardize each numerical feature using its mean and standard deviation in the training dataset. For adversarial training we assume each input x is perturbed by an adversary who is allowed to shift x by a vector δ whose ℓ_∞ -norm is bounded by ε . In particular for a given ε we use the closed-form worst-case perturbation formula in Eq. (12), and we set the ℓ_1 regularization parameter λ to 0.

C.1 Mushroom Dataset

Similar to the plot in Figure 2 for the synthetic dataset, in Figure 9 we show how varying the ε bound on an ℓ_∞ adversary impacts the weight-concentration (measured by Wts.1Pct, defined in Section 6.1) and the AUC, in order to demonstrate that there is a range of ε values that represents a "goldilocks" zone where there is a significant feature-concentration effect while maintaining the (test-set) AUC within 0.01 of the naturally-trained AUC. With adversarial training using $\varepsilon = 1.6$ the Wts.1Pct value is only 12% (compared to almost 97% for a naturally-trained model) while AUC (on natural test data) is 0.99, a drop of only 0.01 compared to a naturally trained model.

As in Figure 3 for the synthetic dataset we also show in Figure 10 how varying the ℓ_1 -regularization strength parameter λ impacts AUC and Wts.1Pct (in natural training, i.e. $\varepsilon = 0$). The figure shows that the highest λ value that maintains an AUC above 0.99 is 600, yet it achieves a Wts.1Pct of around 18%, still significantly higher than the 12% achieved with adversarial training using $\varepsilon = 1.6$.

We now want to show the contrast between the weights learned by natural training and adversarial training with $\varepsilon = 1.6$. Since all features in this dataset are categorical, many with cardinalities close to 10, there are too many features in the "exploded" space to allow a clean display, so we instead look at the aggregate Feature Impact (FI, defined in Eq (26)) over the natural training dataset, see Figure 11. It is worth noting that several features that have a significant impact on the naturally-trained model have essentially no impact on the adversarially trained model. Figures 12 and 13 show the drop-off curves of the feature-weights and FI metrics respectively, and once again it is evident that the drop offs are much steeper with adversarial training compared to natural training.

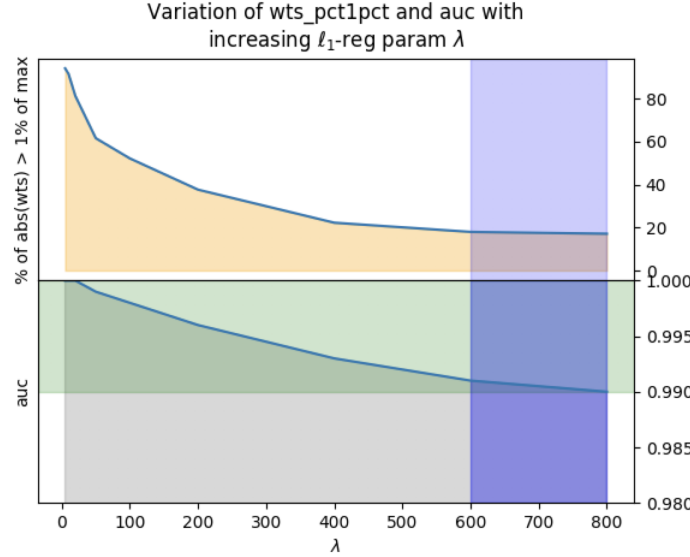


Figure 10: Variation of Wts.1Pct and test AUC for naturally-trained models, with increasing ℓ_1 -regularization parameter λ . Even with a $\lambda = 600$, the Wts.1Pct concentration metric is around 18%, considerably higher than the 12% achieved with adversarial training.

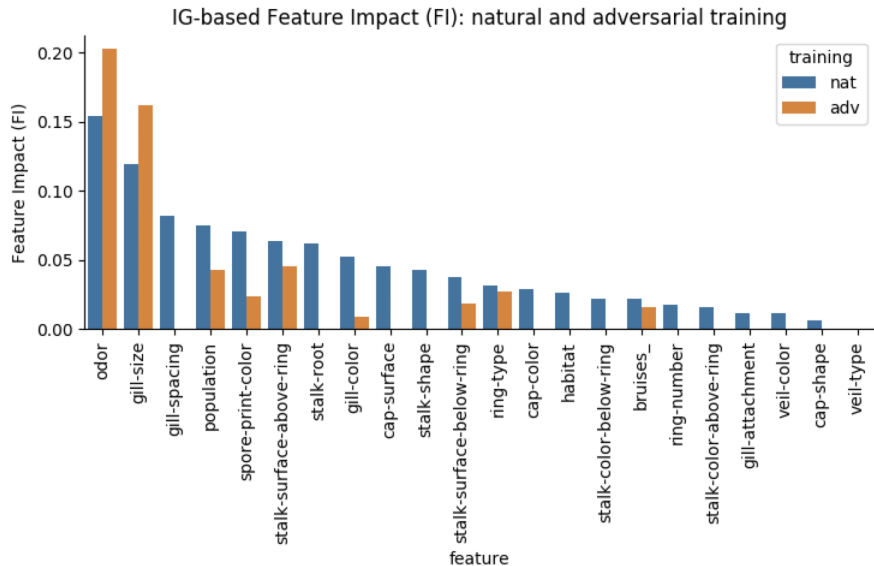


Figure 11: Comparison of aggregate Feature Impact (FI) defined in Eq. (26) for a naturally-trained model, and an adversarially-trained model with $\varepsilon = 1.6$, on the mushroom dataset. The features are arranged left to right in decreasing order of the FI value in the naturally-trained model.

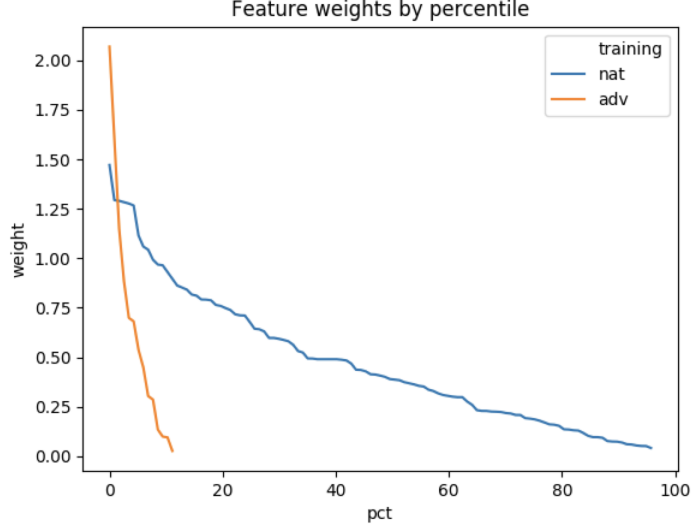


Figure 12: Comparison of drop-off of absolute feature weights in natural and adversarial training, on the mushroom dataset. In each curve, the y -coordinate of a point at percent p equals the feature-weight at the p 'th percentile when the weights are arranged in decreasing absolute value. Both curves are truncated when the weight reaches 1% of the highest weight in the model. The adversarially trained model has a much steeper weight drop-off, with only 12% being above the 1% threshold, compared to 95% with natural training.

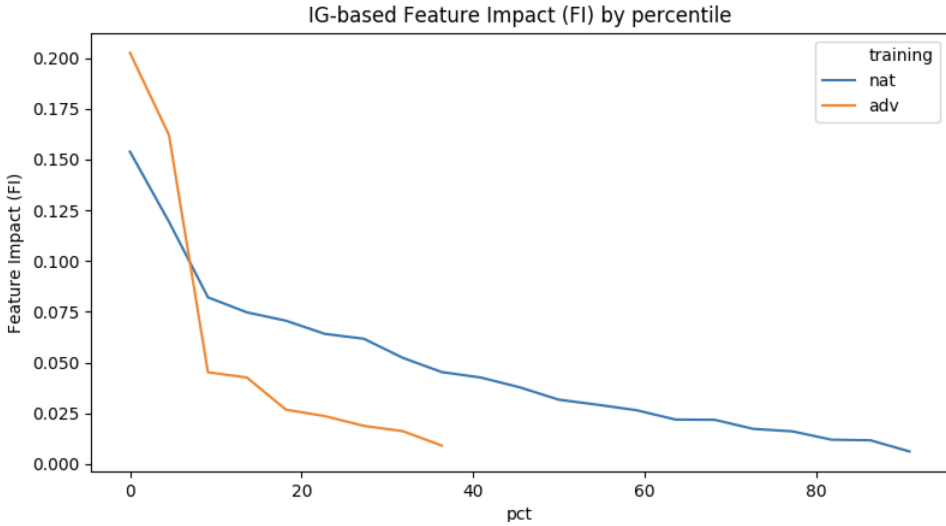


Figure 13: Comparison of drop-off of aggregate Feature Impact FI (measured over the natural training dataset) resulting from natural and adversarial training, for the mushroom dataset. In each curve, the y -coordinate of a point at percent p equals the feature-weight at the p 'th percentile when the weights are arranged in decreasing absolute value. Both curves are truncated when the FI reaches 1% of the highest FI in the model. The adversarially trained model has a much steeper FI drop-off, with only 36% being above the 1% threshold, compared to 90% with natural training.

C.2 Spambase dataset

As with the mushroom dataset, we start by looking at the impact of varying ε (the adversarial ℓ_∞ bound) on the concentration metric Wts.1Pct, see Figure 14. From the chart it is apparent that an adversarially trained model $\varepsilon = 0.6$ achieves a concentration metric Wts.1Pct of around 53% (meaning that 53% of the model's absolute weights are within 1% of the biggest absolute weight), compared to 96% for a naturally-trained model, and yet

yields an AUC (on natural test data) of 0.964, which is no more than 0.01 worse than the AUC of 0.974 for a naturally-trained model.

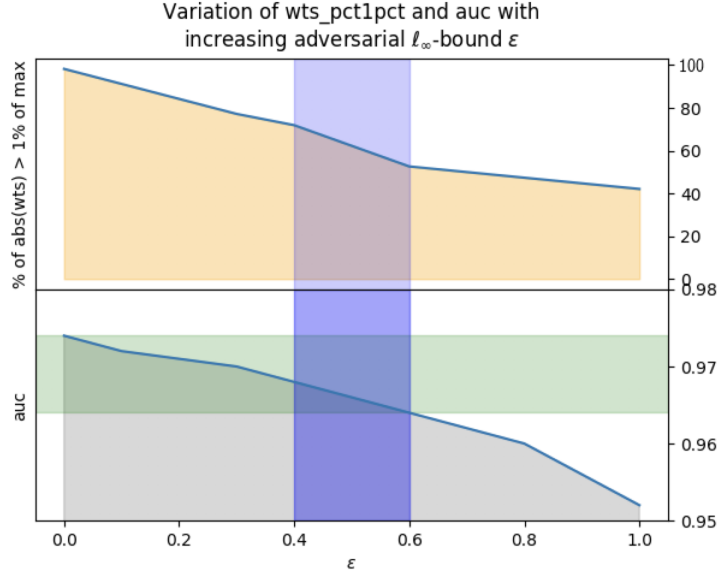


Figure 14: Variation of Wts.1Pct and natural test AUC with increasing ϵ bound on ℓ_∞ perturbations in adversarial training, for the spambase dataset. Note that $\epsilon = 0$ corresponds to natural training, which results in $\text{AUC}=0.974$. The horizontal green band from $\text{AUC}=0.964$ to $\text{AUC}=0.974$ shows the range of AUCs within 0.01 of AUC of the naturally-trained mode. The blue vertical band represents the range of ϵ values (0.4 to 0.6) that are high enough to produce significant model-concentration, yet low enough that AUC is maintained within the green band.

Figure 15 shows that this tradeoff between model-concentration and AUC cannot be achieved by using ℓ_1 -regularization.

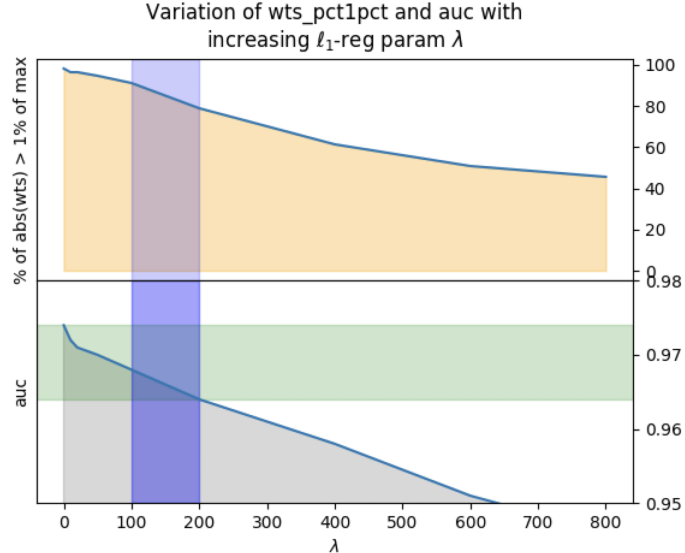


Figure 15: Variation of Wts.1Pct and natural test AUC for naturally-trained models, with increasing ℓ_1 -regularization parameter λ , for the spambase dataset. Even with a $\lambda = 200$, the Wts.1Pct concentration metric is as high as 80% (significantly worse than the 53% for adversarial training), and any higher value of λ pushes the AUC to a level worse than 0.01 below the naturally-trained AUC with no regularization.

We now fix $\varepsilon = 0.6$ for adversarial training and show in Figures 16 and 17 the bar-plots comparing the weights and Feature-Impacts (FI) respectively, between naturally-trained and adversarially-trained models. Since all features are numerical the number of weights is the same as the number of FIs. However the distribution of the FIs does not follow that of the weights.

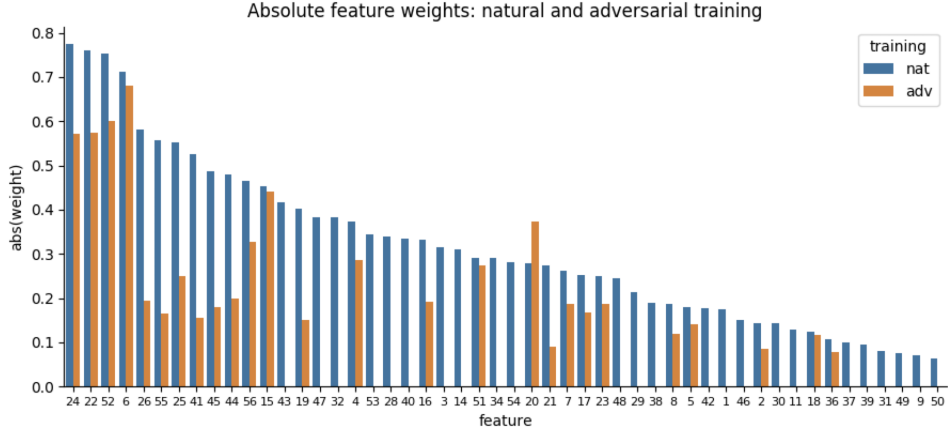


Figure 16: Comparison of absolute model weights for a naturally-trained model, and an adversarially-trained model with $\varepsilon = 0.6$, on the spambase dataset. The features are arranged left to right in decreasing order of their absolute weight in the naturally-trained model. To avoid clutter, we show only features that have an absolute weight at least 8% of the highest weight (across both models). (The features in this figure and the next are identified by integers.)

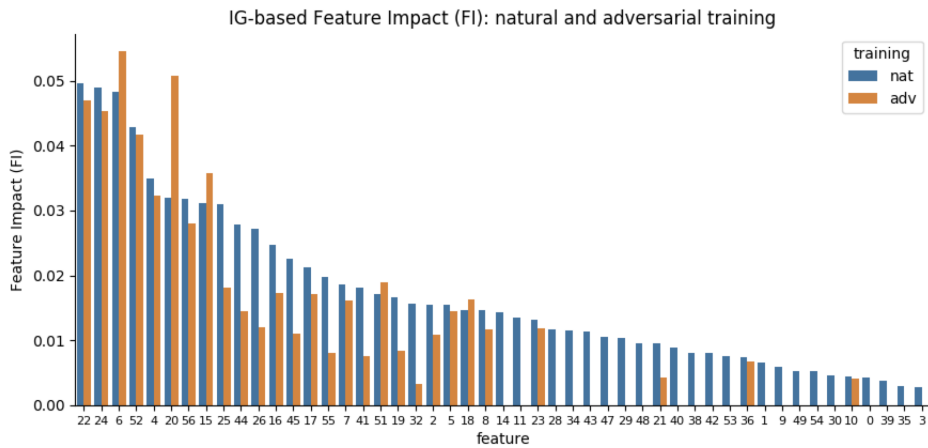


Figure 17: Comparison of aggregate Feature Impact (FI) defined in Eq. (26) for a naturally-trained model, and an adversarially-trained model with $\varepsilon = 0.6$, on the spambase dataset. The features are arranged left to right in decreasing order of their FI in the naturally-trained model. To avoid clutter, we show only features that have an FI at least 5% of the highest FI (across both models).

Figures 18 and 19 contrast the drop-off curves of feature-weights and Feature Impacts (FI) respectively between naturally-trained and adversarially-trained models.

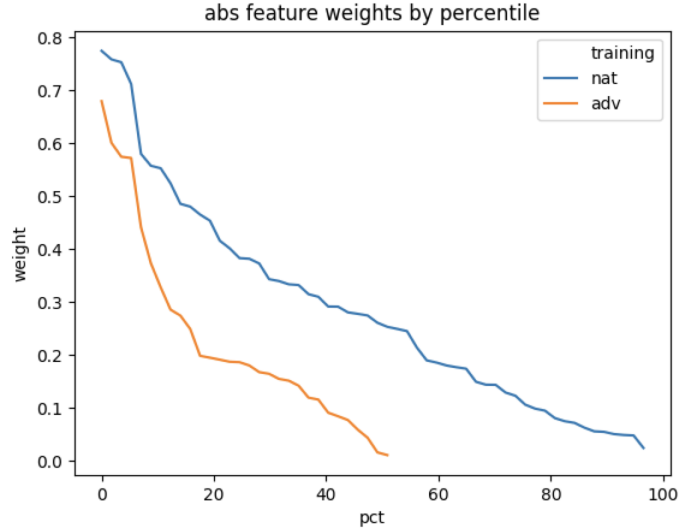


Figure 18: Comparison of drop-off of absolute feature weights in natural and adversarial training, for the spambase dataset. In each curve, the y -coordinate of a point at percent p equals the feature-weight at the p 'th percentile when the weights are arranged in decreasing absolute value. Both curves are truncated when the weight reaches 1% of the highest weight in the model. The adversarially trained model has a much steeper weight drop-off, with only 52% being above the 1% threshold, compared to 96% with natural training.

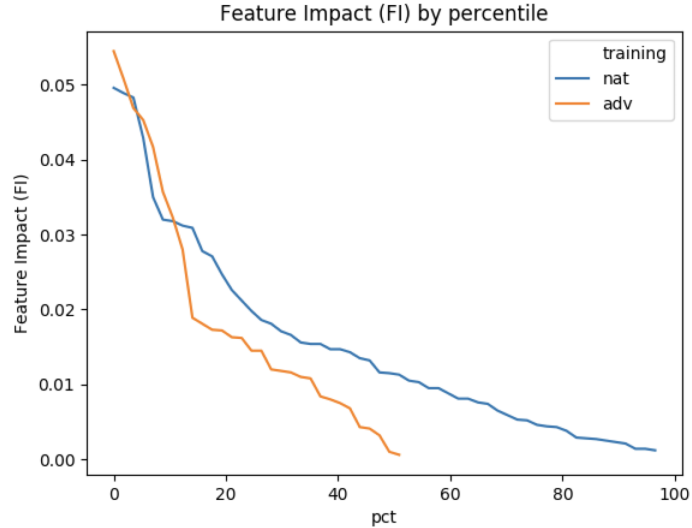


Figure 19: Comparison of drop-off of aggregate Feature Impact (FI) (computed over the natural training dataset) for a naturally-trained and adversarially-trained model. In each curve, the y -coordinate of a point at percent p equals the feature-weight at the p 'th percentile when the weights are arranged in decreasing absolute value. Both curves are truncated when the FI reaches 1% of the highest FI in the model. The adversarially trained model has a much steeper FI drop-off, with only 52% being above the 1% threshold, compared to 96% with natural training.